

2004

# Unusual separations with macrocyclic glycopeptide chiral stationary phases and chromatographic analysis and characterization of microbes

Bo Zhang  
Iowa State University

Follow this and additional works at: <https://lib.dr.iastate.edu/rtd>

 Part of the [Analytical Chemistry Commons](#)

## Recommended Citation

Zhang, Bo, "Unusual separations with macrocyclic glycopeptide chiral stationary phases and chromatographic analysis and characterization of microbes " (2004). *Retrospective Theses and Dissertations*. 829.  
<https://lib.dr.iastate.edu/rtd/829>

This Dissertation is brought to you for free and open access by the Iowa State University Capstones, Theses and Dissertations at Iowa State University Digital Repository. It has been accepted for inclusion in Retrospective Theses and Dissertations by an authorized administrator of Iowa State University Digital Repository. For more information, please contact [digirep@iastate.edu](mailto:digirep@iastate.edu).

**Unusual separations with macrocyclic glycopeptide chiral stationary phases and chromatographic analysis and characterization of microbes**

by

**Bo Zhang**

A dissertation submitted to the graduate faculty  
in partial fulfillment of the requirements for the degree of

**DOCTOR OF PHILOSOPHY**

Major: Analytical Chemistry

Program of Study Committee:  
Daniel W. Armstrong, Major Professor  
Maohong Fan  
Robert S. Houk  
Jacob W. Petrich  
Walter S. Trahanovsky

Iowa State University

Ames, Iowa

2004

Copyright © Bo Zhang, 2004. All rights reserved.

UMI Number: 3136362

### INFORMATION TO USERS

The quality of this reproduction is dependent upon the quality of the copy submitted. Broken or indistinct print, colored or poor quality illustrations and photographs, print bleed-through, substandard margins, and improper alignment can adversely affect reproduction.

In the unlikely event that the author did not send a complete manuscript and there are missing pages, these will be noted. Also, if unauthorized copyright material had to be removed, a note will indicate the deletion.

**UMI**<sup>®</sup>

---

UMI Microform 3136362

Copyright 2004 by ProQuest Information and Learning Company.

All rights reserved. This microform edition is protected against unauthorized copying under Title 17, United States Code.

ProQuest Information and Learning Company  
300 North Zeeb Road  
P.O. Box 1346  
Ann Arbor, MI 48106-1346

Graduate College  
Iowa State University

This is to certify that the doctoral dissertation of  
**Bo Zhang**  
has met the dissertation requirements of Iowa State University

Signature was redacted for privacy.

**Major Professor**

Signature was redacted for privacy.

**For the Major Program**

## TABLE OF CONTENTS

<b>PART I. UNUSUAL SEPARATIONS WITH MACROCYCLIC GLYCOPEPTIDE CHIRAL STATIONARY PHASES</b>	<b>1</b>
<b>CHAPTER 1. INTRODUCTION</b>	<b>2</b>
References	6
<b>CHAPTER 2. REVERSAL OF ENANTIOMERIC ELUTION ORDER ON MACROCYCLIC GLYCOPEPTIDE CHIRAL STATIONARY PHASES</b>	<b>7</b>
Abstract	7
Introduction	7
Experimental	10
Materials	10
Methods	10
Results and discussion	11
References	17
<b>CHAPTER 3. SELECTIVE SEPARATIONS OF PEPTIDES WITH SEQUENCE DELETIONS, SINGLE AMINO ACID POLYMORPHISMS, AND/OR DIASTEREOMERS USING A TEICOPLANIN LC STATIONARY PHASE</b>	<b>19</b>
Abstract	19
Introduction	20
Materials.	22
Instrument.	25
Methods	25
Results and Discussion	25
Peptide separations	25
Separation of Peptides containing single amino acid polymorphism (SAAP)	28
Optimization of Peptide Separations on Chirobiotic Stationary Phases	33
Organic Modifier Content and Retention Behavior	33
Mobile phase pH	35
Electrospray-Mass Spectrometry Detection	38
Conclusions	42
Acknowledgements	42
References	42
<b>PART II. CHROMATOGRAPHIC ANALYSIS AND CHARACTERIZATION OF MICROBES</b>	<b>45</b>
<b>CHAPTER 4. INTRODUCTION</b>	<b>46</b>
References	48

<b>CHAPTER 5. FACILE MONITORING AND EVALUATION OF BACTERIA IN A FERMENTATION PROCESS USING PERFUSION CHROMATOGRAPHY AND POLARIMETRY DETECTION</b>	<b>50</b>
Abstract	50
1 Introduction	51
2 Material and methods	53
2.1 Chemicals	53
2.2 Spherical monodisperse porous packing for perfusion chromatography	53
2.3 Biochemicals	53
2.4 Column preparation	54
2.5 Culturing bacteria	54
2.6 Chromatographic system	55
2.7 Polarimeter detector	55
3 Sieving by close-packed hard spheres	55
3.1 Comparing sizes	55
3.2 The close-packing of spheres	56
3.3 Properties of columns closely packed with non-porous uniform spheres	61
4 Evaluation of the perfusion column	63
4.1 Molecules and polymers	64
4.2 Bacteria	65
Conclusions	70
Acknowledgments	71
References	71
<b>CHAPTER 6. PORE EXCLUSION CHROMATOGRAPHY-INDUCTIVELY COUPLED PLASMA-MASS SPECTROMETRY FOR MONITORING ELEMENTS IN BACTERIA: A STUDY ON MICROBIAL REMOVAL OF URANIUM FROM AQUEOUS SOLUTION</b>	<b>73</b>
Abstract	73
1 Experimental section	75
1.1 Chemicals and Materials	75
1.2 Bacteria Growth and Counting	76
1.3 Pore Exclusion/Size Exclusion Chromatography	77
1.4 ICPMS and Sample Introduction	78
2 Results and discussion	78
2.1 Chromatograms	78
2.2 Impact of Uranium on Cell Growth	81
2.3 Extrinsic versus Intrinsic Uranium	83
2.4 Atomization of Cells in the ICP	84
Conclusions	86
Acknowledgments	86
References	87
<b>GENERAL CONCLUSIONS</b>	<b>90</b>
<b>ACKNOWLEDGEMENTS</b>	<b>93</b>

**PART I. UNUSUAL SEPARATIONS WITH MACROCYCLIC  
GLYCOPEPTIDE CHIRAL STATIONARY PHASES**

## CHAPTER 1. INTRODUCTION

The development of widely useful, high-efficiency enantiomeric separations is a tremendous success story. In a little more than a decade (starting in the early 1980s), this field went from an academic curiosity to an extraordinarily useful collection of related techniques, which are routinely used today in many branches of science and technology. Indeed, the U.S. Food and Drug Administration (FDA) issued guidelines for the development of stereoisomeric drugs in 1992[1] largely because of the tremendous advances in enantiomeric separations that facilitated enantioselective pharmacokinetic and pharmacodynamic studies, as well as rapid, sensitive chiral assays. This completely altered the nature of chiral drug development.

Today, the FDA may be considering additional guidelines in this area [2]. In addition, greater attention is being paid to the stereochemical properties of compounds in foods, fragrances, agrochemicals, and the natural and work environments. Enantiomeric impurities are now measured routinely to the 0.01% level. HPLC can be used to measure an amino acid enantiomeric impurity near the parts-per-million level[3,4].

Chiral selectors can be classified in many different ways. One of the more useful classification formats is by structure (Table 1). Knowing the structure and properties of a chiral selector is the first step in understanding how they function and what they will separate. Chiral selectors also can be classified according to their source or origin (Table 1). Today, the semisynthetic chiral selectors dominate the field of enantiomeric separations, although many important contributions are still made (particularly in LC) by natural and synthetic compounds.



Table 1. Structure-based classification and origin of chiral selectors

Class*	Examples
Macrocyclic	Cyclodextrins and their derivatives, glycopeptides (macrocyclic antibiotics), and chiral crown ethers
Polymeric	Naturally occurring (derivatized linear or branched carbohydrates and proteins) and synthetic polymers
$\pi$ - $\pi$ Association	$\pi$ -Electron acceptor ( $\pi$ -acid), $\pi$ -electron donator ( $\pi$ -base), and combination types (containing both p-electron acceptor and donator groups)
Ligand exchange (bidentate)	Hydroxyproline, penicillamine
Miscellaneous and hybrid	Cross-linked tartaric acid derivatives
Origin	Examples
Naturally occurring	Cyclodextrins, macrocyclic glycopeptides, amino acids, and proteins
Semisynthetic	Derivatized cyclodextrins, derivatized linear carbohydrates, modified macrocyclic glycopeptides, derivatized amino acids and alkaloids (with $\pi$ -acid or $\pi$ -basic groups), and tartaric acid derivatives
Synthetic chiral selectors	Methacrylate polymers, a few $\pi$ - $\pi$ complex compounds, and chiral crown ethers

\*Pertinent references for each class and type of chiral selector can be found in Refs. 5 and 6.

Attempts to classify chiral selectors on the basis of perceived function were somewhat arbitrary because a single type of chiral selector can function differently in different situations and environments. For example, the Cyclobond-I-SN (i.e.,  $\beta$ -cyclodextrin functionalized with *S*-naphthylethylcarbamate groups) chiral stationary phase (CSP) can form inclusion complexes in the reversed-phase (RP) mode, act as a  $\pi$ -complex CSP in the normal-phase (NP) mode, or show only external surface adsorption in the polar organic (PO) mode. In a few cases, the structure and exact function of a chiral selector is not well understood.

Arguably, the macrocyclic class of chiral selectors has had the biggest impact on analytical enantiomeric separations. The vast majority of all GC and CE enantiomeric separations are done with macrocyclic chiral selectors, predominantly derivatized cyclodextrins. However, in LC, the field is much more divided. Early on, the macrocyclic and protein-based CSPs were used for the majority of RP and PO mode separations, while the derivatized carbohydrates and  $\pi$ -complex CSPs were used for the majority of NP separations. More recently, these lines have blurred. For example, the macrocyclic glycopeptide and aromatic-derivatized cyclodextrins are highly effective in the NP mode, while some of the linear derivatized carbohydrate CSPs have been conditioned to work in the RP mode (they've also been shown to work in the PO mode).

Since the advent of commercial CSPs, there have always been a few "dominant" columns that accomplished the majority of separations. These so-called preferred columns have evolved or changed with time as new and better CSPs have been developed. In 1985, for example, three of the best columns were based on 3,5-dinitrobenzoylphenylglycine (Regis's phenylglycine),  $\beta$ -cyclodextrin (Astec's Cyclobond I), and  $\alpha_1$ -acid glycoprotein (LKB). Of course, there were far fewer choices at that time. By 1990, the Daicel Chiracel OD (3,5-dimethylphenylcarbamolated cellulose) proved to be the most widely applicable of the cellulosic columns, and the Crownpak chiral crown ether column's broader selectivity and ease of use were favored for amino acid separations.

Also at this time, derivatized cyclodextrin CSPs (Cyclobond I-RSP, Cyclobond I RN, etc.), a more stable and efficient second-generation  $\alpha_1$ -acid glycoprotein column (ChromTech's Chiral AGP), and new  $\pi$ - $\pi$  association CSPs with better selectivity became available. By 1995, the newest chiral selectors, macrocyclic glycopeptides (i.e., the

Chirobiotic series from Astec), were having a significant impact because of their wide utility and high efficiency. Also, the most broadly useful  $\pi$ -complex CSP (Whelk-O 1 from Regis) and the most widely useful derivatized linear carbohydrate CSP (Chiralpak AD from Daicel) were introduced around this time.

It is only when these few "mainstays" don't work that the sometimes arduous task of surveying the vast array of other columns presents itself. Sometimes enantiomeric separations can be achieved on two or more CSPs. This added flexibility increases the possibility that analysts can achieve a separation under their preferred experimental conditions and with the desired efficiency, selectivity, and run time.

As a class of chiral selectors, vancomycin, teicoplanin, and ristocetin A are similar, structurally related molecules. Thus, they have somewhat similar, but not identical selectivities. Reversing the enantioselectivity of a separation on these CSPs is difficult, and would be considered unusual. The investigation of reversal of elution orders on these stationary phases is the first part of this dissertation.

As stated above, macrocyclic glycopeptides chiral stationary phases are widely utilized for enantiomeric separations, including amino acids, dipeptides, and tripeptides[5,6]. They are known to selectively bind specific amino acids and sequences of amino acids via electrostatic and hydrogen bonding interactions[6,7]. It is highly likely that they also are selective for closely related but non-enantiomeric peptides of any chain length. Their separation mechanism, and therefore selectivity, is significantly different from both reversed phase and ion-exchange LC. Some physiologically important peptides were studied by using these stationary phases as discussed in this dissertation.

**References**

- (1) U.S. Food and Drug Administration. *Chirality* 1992, 4, 338-340.
- (2) Miller, S. P., FDA Perspective on Quality Control for Chiral Pharmaceuticals.  
Abstract and Presentation at ISCD 13, Chirality 2001, Orlando, FL, July, 2001.
- (3) Armstrong, D. W., Lee, J. T., Chang, L. W. *Tetrahedron Asymmetry* 1998, 9, 2043-2064.
- (4) Armstrong, D. W., He, L., Yu, T., Lee, J. T., Liu, Y. -S. *Tetrahedron Asymmetry* 1999, 10, 36-60.
- (5) Péter, A., Török, G., Armstrong, D.W. *J. Chromtogr.* 793 (1998) 283.
- (6) Berthod, A., Liu, Y., Bagwill, C., Armstrong, D.W., *J. Chromtogr.* 731 (1996) 123.
- (7) Péter, A., Török, G., Armstrong, D.W., Tóth, G., Tourwé, D., *J. Chromtogr. A* 904 (2000) 1.

## CHAPTER 2. REVERSAL OF ENANTIOMERIC ELUTION ORDER ON MACROCYCLIC GLYCOPEPTIDE CHIRAL STATIONARY PHASES

A paper published in *Journal of Liquid Chromatography & Related Technologies*

T.L. Xiao<sup>1</sup>, B. Zhang<sup>1</sup>, J.T. Lee<sup>2</sup>, F. Hui<sup>3</sup>, D.W. Armstrong\*<sup>1</sup>

<sup>1</sup> Department of Chemistry, Iowa State University, Ames, IA 50011

<sup>2</sup> Advanced Separation Technologies, Inc., Whippany, NJ 07981

<sup>3</sup> Laboratoire Environnement et Chimie Analytique, CNRS ERS657, ESPCI, 75005 Paris, France

### Abstract

The macrocyclic glycopeptides, vancomycin, teicoplanin, and ristocetin A are naturally occurring chiral molecules that have been developed into one of the most useful classes of chiral stationary phases (CSPs) for HPLC. Since these chiral selectors are structurally related, they tend to have similar, but not identical, enantioselectivities for most compounds. CSPs, of this type, with opposite enantioselectivities are rare. Two exceptions have been found to this. The oxazolidiones (starting materials for asymmetric synthesis) and dansyl amino acids all show a reversal in enantioselective retention on one of these three related CSPs. By using the HPLC assays developed for these compounds, the levels of enantiomeric impurities can be measured down to  $\sim 0.01\%$ . The enantiomeric purity of commercial oxazolidiones was determined.

### Introduction

The aglycone portion of all the macrocyclic glycopeptides contain either three or four fused macrocyclic rings (Figure 1). Together, these fused rings form a semirigid basket-

shaped entity. Each aglycone basket has associated with it: an amine moiety, a carboxylic acid group (which is esterified in ristocetin A) and phenolic moieties. These groups, along with an amino-saccharide, control the charge of these molecules. In addition, the aglycone contains several amide or peptide bonds (Figure 1). Each aglycone has one or more carbohydrate moieties attached at various locations. A single disaccharide is attached to vancomycin, while teicoplanin has three monosaccharides associated with it (Figure 1). Compared to the aglycone portion of these molecules, the carbohydrate moieties are relatively free to alter their orientation.

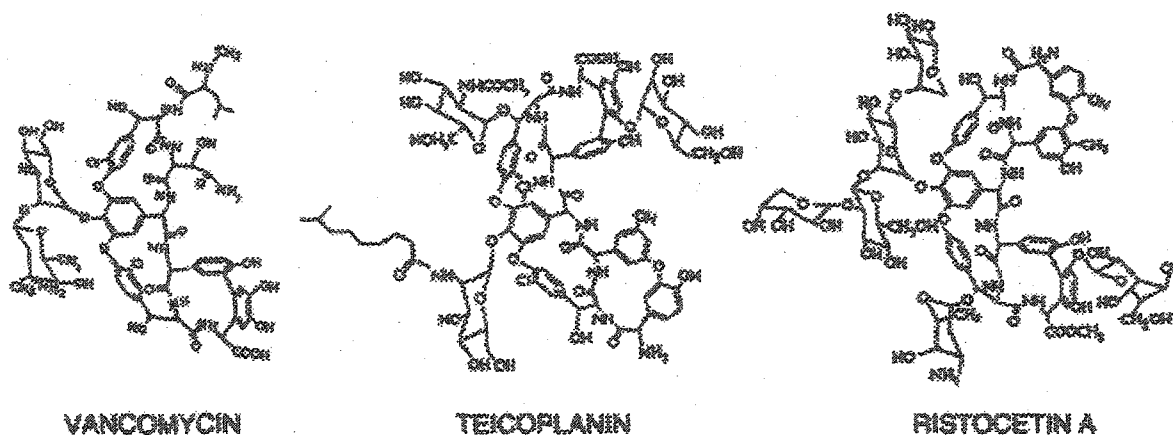


**Figure 1.** Schematic showing the structures of the related macrocyclic glycopeptides: vancomycin, teicoplanin, and ristocetin A.

As a class of chiral selectors, the macrocyclic glycopeptides have very broad enantioselectivity, and can be used in all chromatographic modes (i.e., reversed phase, normal phase and polar organic modes). The teicoplanin-based CSP (Chirobiotic T) is now the preferred means of resolving native amino acids (both natural and synthetic types). (1), (5), (9-10) A distinct amino acid and carboxylic acid binding site has been identified for

these related macrocycles. (5), (7), (24) Furthermore, it appears that there are other binding sites for neutral and cationic chiral analytes. (24)

Clearly, vancomycin, teicoplanin, and ristocetin A are similar, structurally related molecules. They have the same biological function, which is to bind to D-alanyl-alanine moieties in the cell wall of Gram positive bacteria. (1-3), (8) Although they are related, these macrocycles are far from being identical. Thus, they have somewhat similar, but not identical selectivities. This property gave rise to the operating “principle of complimentary separations.” This means that if only a partial enantioseparation can be obtained on one CSP, then it is likely that a baseline separation will be achieved on one of the related CSPs. (4), (6)

Given the similarities of the glycopeptide chiral selectors, it is not surprising that enantiomeric elution order appears to be the same on all of these CSPs. Since these macrocyclic glycopeptides are complex, natural molecules, their enantiomers are unavailable. Consequently, reversing the enantioselectivity of a separation on these CSPs is difficult, and would be considered unusual. After performing thousands of separations on these CSPs over the last few years, we have found a few cases in which the enantioselectivity of a separation could be reversed either by using a related glycopeptide CSP or, in one case, by altering the mobile phase composition. This behavior has not been reported previously for this class of CSPs.

## Experimental

### *Materials*

The HPLC-grade solvents [methanol, reagent alcohol, acetonitrile, glacial acetic acid, triethylamine (99+% pure) and hexane] were purchased from Fisher Scientific (Fair Lawn, NJ, USA). All racemates and single enantiomers of derivatized amino acids and neutral molecules used in this study were purchased from Aldrich (Milwaukee, WI, USA) and Fluka (Milwaukee, WI, USA). All HPLC Chirobiotic columns [Chirobiotic V (vancomycin), Chirobiotic T (teicoplanin), Chirobiotic R (ristocetin A)] were (stainless-steel 25 cm × 4.6 mm) obtained from Advanced Separation Technologies, Inc. (Whippany, NJ).

### *Methods*

The separations were performed on Shimadzu (Columbia, MD) HPLC systems equipped with Model LC-6A pumps, Model SPD-6A, and SPD-6AV UV detectors, SCL-6A and SCL-6B system controllers, CR-601 and C-R3A Chromatopac integrators, and Rheodyne (Cotati, CA, USA) manual injectors. All samples were dissolved in methanol with concentration of 1 mg/mL and all separations were achieved at room temperature (~22°C).

Mobile phases were prepared by mixing the indicated volumes of solvents or deionized and filtered water and degassed with a Crest Ultrasonic sonicator (Trenton, NJ, USA). The HPLC mobile phase flow rate was 1 mL/min and UV detection wavelengths were 254 nm for compounds containing aromatic rings and 220 nm for all others. The pH value of buffer mobile phase was measured with an Orion (Boston, MA, USA) pH meter Model 410A. Elution orders were determined by spiking a single pure enantiomer into the solution of the corresponding racemic compound.



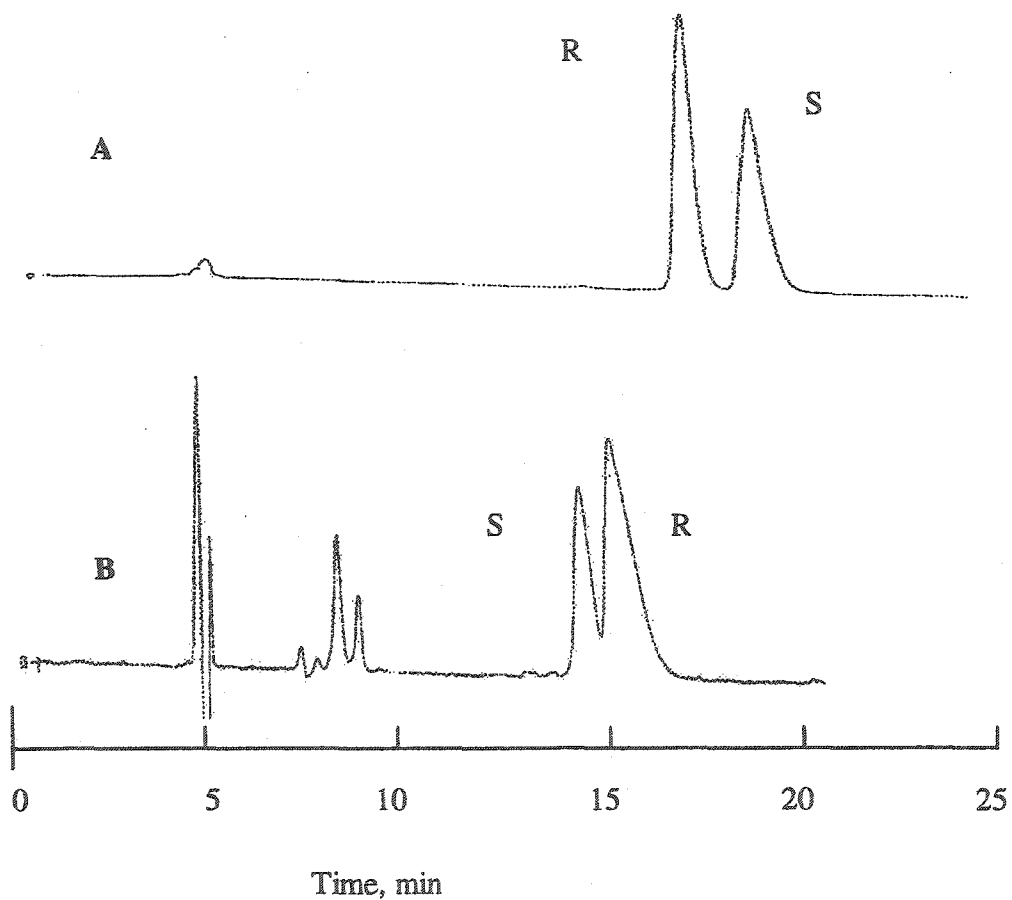
## Results and discussion

There are few reports on the reversal of enantiomeric retention on CSPs containing natural chiral selectors. (25-26) These CSPs usually are either protein-based or linear derivatized carbohydrates. (25-26) The reversal of enantiomeric elution usually was the result of a change in mobile phase composition, although temperature effects also could be relevant. A solvent induced conformational change in the chiral selector often was given as the reason for the change in selectivity. Note, that the changes in solvent composition that were reported were not drastic changes, such as going from the reversed phase mode to the normal phase mode (where the mechanism changed). Rather, they are milder changes, such as altering the organic modifier type or altering the pH in a reversed phase separation.

The macrocyclic glycopeptides are much smaller than the biological polymers that are used as chiral selectors. Thus, they seem to be less susceptible to solvent-induced changes in enantioselectivity. Indeed, the only reverse in enantioselective retention we've documented on the vancomycin CSP (involving different mobile phases), was for N-benzyl- $\alpha$ -methylbenzylamine (Figure 2). In this case, it took a rather drastic change in the mobile phase (i.e., from the polar organic mode to the reversed phase mode). It is less surprising to get a change in enantioselectivity if the retention mechanism is completely altered. Despite this fact, the enantiomeric retention order of a wide variety of solutes on the macrocyclic glycopeptide CSPs is reasonably constant. Table 1 lists several classes of molecules that appear to have the same basic enantioselectivity on the vancomycin, teicoplanin, and ristocetin chiral stationary phases.

**Table 1.** Some Classes of Compounds That Appear to Have the Same Enantiomeric Retention Order on Chirobiotic V, T, and R Chiral Stationary Phases.

- 
1. FMOC-amino acids
  2. N-t-BOC-amino acids
  3. N-CBZ-amino acids
  4. Nonsteroidal antiinflammatory compounds
  5.  $\beta$ -adrenergic blockers
  6. 4-aryldihydropyrimidines
- 

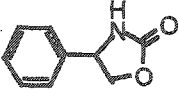
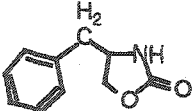
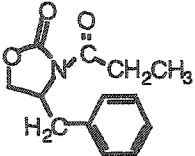
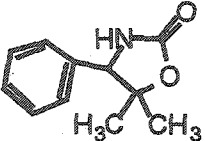
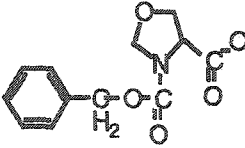
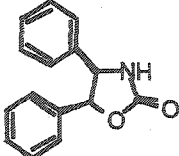


**Figure 2.** Chromatograms showing the reversal in elution order for enantiomers of N-benzyl- $\alpha$ -methylamine on the Chirobiotic V column (250 x 4.6 mm) resulting from a change in the mobile phase composition. Chromatogram (A) was generated in the polar organic mode (Acetonitrile/0.1% TEAA buffer, pH 4.1; 20/80, by volume).

Throughout the course of our studies, it was noted that a compound would sometimes have a different enantiomeric retention order on one of the macrocyclic glycopeptides CSPs. Thus far, all compounds that have shown this behavior fall into one of two classes: 1) the oxazolidinones, and 2) dansylated amino acids (Table 2, Table 3). Of these, the dansyl-amino acids show the most consistent behavior. The D-enantiomers are preferentially retained on the vancomycin and teicoplanin CSPs, while the L-enantiomer is more retained on the ristocetin CSP (Table 2, Table 3). It is the retention order on the ristocetin CSP that is unusual or anomalous. In most other cases, both the native and derivatized D-amino acids enantiomers are more retained on macrocyclic glycopeptide CSPs. Indeed, the biological function of these glycopeptides is to bind to D-alanyl-D-alanine on bacterial cell walls. The dansyl-fluorophore is a relatively bulky group and it contains an amine functionality. Apparently, this combination of additional steric-bulk and the hydrogen bonding or charge effect of the amine is sufficient to alter the enantioselectivity of ristocetin A, toward dansyl amino acids.

It is known that amino acids associate with the amine moiety these macrocyclic glycopeptides via their carboxylic acid groups. (1), (5), (9-10) This association can be either electrostatic in nature or hydrogen bonding depending on the pH and/or mobile phase composition. The additional simultaneous interactions (required for chiral recognition) are thought to consist of hydrogen bonds to the amide groups of the aglycone, and in some cases, hydrophobic interactions (at least in the reversed-phase mode). Derivatizing the amine group of an amino acid with a fluorophore can alter the secondary interactions between the analyte and the aglycone. For example, the amino moiety of the amino acid would no longer be available for hydrogen bonding to the macrocyclic glycopeptide. However, the steric bulk of

**Table 2.** Members of compound oxazolidinones where there is a change in the enantiomeric elution order on macrocyclic glycopeptide CSPs.

Compound Oxazolidinones	Structure	Elution order <sup>a</sup>			Mobile Phase <sup>b</sup>
		Vancomycin V	RistocetinA R	Teicoplanin T	
RS- 4- phenyl- 2-oxazolidinone		R	S	R	T& R= 100% MeOH V=H <sub>2</sub> O/MeOH(90/10)
RS- 4- benzyl- 2-oxazolidinone		R	S	R	T=100% MeOH V=H <sub>2</sub> O/MeOH(90/10) R=H <sub>2</sub> O/MeOH(75/25)
RS- 4- benzyl- 3-propionyl-oxazolidinone		R	Unresolved	S	T=Buffer <sup>c</sup> /MeOH (90/10) V=MeOH/H <sub>2</sub> O(82/18)
RS- 5,5-dimethyl-4-phenyl-2-oxazolidinone		R	S	R	V, R, T = Hex/EtOH(80/20)
RS-3-benzyloxy carbonyl-4-oxazolidine carboxylic acid		R	R	S	T=Buffer/MeOH (80/20) R=Buffer/MeOH (80/20) V= EtOH/H <sub>2</sub> O(40/60)
4S,5R(+)- cis- 4,5-diphenyl-2-oxazolidinone		4R,5S	4S,5R	4S,5R	V, R, T =EtOH/Hex(50/50)

<sup>a</sup> The configuration of the first eluted enantiomer is given.

<sup>b</sup> The flow rate for all separation was 1.0 ml/min except for the first two compounds in this table which was 0.5 ml/min.

<sup>c</sup> The buffer was 1% triethylamine acetate, pH= 4.1.

Table 3. Members of compound dansylated amino acids where there is a change in the enantiomeric elution order on macrocyclic glycopeptide CSPs.

Dansyl-Amino acid	Structure	Elution order <sup>a</sup>			Mobile Phase <sup>b</sup>
		Vancomycin V	RistocetinA R	Teicoplanin T	
DL - Valine		L	D	L	Buffer <sup>b</sup> /MeOH (80/20)
DL - Threonine		L	D	L	Buffer/MeOH (80/20)
DL - Glutamic acid		L	D	L	Buffer/MeOH (80/20)
DL - Aspartic acid		L	D	L	Buffer/MeOH (80/20)
DL - Serine		L	D	L	Buffer/MeOH (80/20)
DL - Phenylalanine		L	D	L	Buffer/MeOH (80/20)
DL - Tryptophan		unresolved	D	L	Buffer/MeOH (80/20)
DL - Methionine		L	D	L	Buffer/MeOH (80/20)
DL - Norvaline		L	D	L	Buffer/MeOH (80/20)

the fluorophore could accentuate either hydrophobic interaction (in the reversed phase mode) or steric repulsive interactions. As mentioned previously, the dansyl group also contains an amine moiety that could result in additional interactions.

The oxazolidinones do not show consistent retention behavior, as do the dansyl-amino acids (Table 2, Table 3). It is not known how the oxazolidinones interact with the macrocyclic glycopeptides. Hence, the relative retentions reported can only be taken as empirical observations. The R-enantiomer always elutes before the S-enantiomer on the vancomycin CSP. However, there was no consistent pattern on either the ristocetin A or teicoplanin CSPs.

Chiral oxazolidinones are widely used in asymmetric synthesis. Since they are commercially available starting materials, it is often assumed that they are enantiomerically pure. In previous work, it was shown that enantiomeric impurities were prevalent in most of the available chiral catalysts, auxiliaries, synthons, and resolving agents. (27) Table 4 gives the enantiomeric purity found for the oxazolidinones used in this study. Note the wide variation in the enantiomeric purity found for this class of chiral compounds. As was noted previously, the batch-to-batch enantiomeric purity of each of these commercial chiral auxiliaries varies widely, since there is no enantiomeric quality control in their production or sale. (26-27)

Table 4. The enantiomeric composition of chiral compounds which show reversal in enantiomer elution order.

Compound name	Commercial source	Enantiomeric composition		Separation Method number <sup>a</sup>
		Enantiomeric contaminant(%)	Enantiomeric excess(%)	
RS-4-phenyl-2-oxazolidinone	Aldrich	S=0.05 R=0.20	R=99.90 S=99.60	1
RS-4-benzyl-2-oxazolidinone	Aldrich	S=0.06 R=0.03	R=99.88 S=99.94	2
RS-4-benzyl-3-propionyl-oxazolidinone	Aldrich	S=0.30 R=0.14	R=99.40 S=99.72	3
RS-5,5-dimethyl-4-phenyl-2-oxazolidinone	Aldrich	R=0.03 S=0.08	S=99.94 R=99.84	4
RS-3-benzyloxy carbonyl-4-oxazolidinone carboxylic acid	Aldrich	S=2.38 R=0.85	R=95.24 S=98.30	5
4S,5R(+)-cis-4,5-diphenyl-2-oxazolidinone	Aldrich			

<sup>a</sup> Method No. 1 = Chirobiotic T. Mobile phase 1% TEAA/MeOH=80/20(pH=4.1), Flow rate 1ml/min. Method No. 2 = Chirobiotic T. Mobile phase 1% TEAA/MeOH=90/10(pH=4.1), Flow rate 1m. Method No. 3 = Chirobiotic T. Mobile phase 1% TEAA/MeOH=85/15(pH=4.1), Flow rate 1ml/min. Method No. 4 = refer to D. W. Armstrong et al./ Tetrahedron: Asymmetry 9 (1998) 2043-2064. Method No. 5 = Chirobiotic T<sub>AG</sub>. Mobile phase 1% TEAA/MeOH=70/30(pH=4.1), Flow rate 1ml/min.

## References

1. D.W. Armstrong, Y. Tang, S. Chen, Y. Zhou, C. Bagwill, J.-R. Chen. *Anal. Chem.*, **66**, 1473, (1994).
2. D.W. Armstrong, K.L. Rundlett, J.-R. Chen. *Chirality*, **6**, 496, (1994).
3. D.W. Armstrong, Y. Liu, K.H. Ekborg-Ott. *Chirality*, **7**, 474, (1995).
4. S. Chen, Y. Liu, D.W. Armstrong, P. Victory, B. Martinez-Teipel. *J. Liq. Chromatogr.*, **18**, 1495, (1995).
5. A. Berthod, Y. Liu, C. Bagwill, D.W. Armstrong. *J. Chromatogr. A*, **731**, 123, (1996).
6. M.P. Gasper, A. Berthod, U.B. Nair, D.W. Armstrong. *Anal. Chem.*, **68**, 2501, (1996).
7. U.B. Nair, S.S.C. Chang, D.W. Armstrong, Y.Y. Rawjee, D.S. Eggleston, J. V. McArdle. *Chirality*, **8**, 590, (1996).
8. K.H. Ekborg-Ott, Y. Liu, D.W. Armstrong. *Chirality*, **10**, 434, (1998).

9. A. Peter, G. Torok, D.W. Armstrong. *J. Chromatogr. A*, **793**, 283, (1998).
10. A. Peter, G. Torok, D.W. Armstrong, G. Toth, D. Tourwe. *J. Chromatogr. A*, **828**, 177, (1998).
11. K.B. Joyce, A.E. Jones, R.J. Scott, R.A. Biddlecombe, S. Pleasance. *Rapid Commun. Mass Spec.*, **12**, 1899, (1998).
12. K.M. Fried, P. Koch, I.W. Wainer. *Chirality*, **10**, 484, (1998).
13. H.Y. Aboul-Enein, V. Serignese. *Chirality*, **10**, 358, (1998).
14. E. Tesarova, A. Bosakova, V. Pacakov. *J. Chromatogr. A*, **838**, 121, (1999).
15. Q. Sun, S.V. Olesik. *Anal. Chem.*, **71**, 2139, (1999).
16. J. Lehotay, K. Hrobonová, J. Krupcik, J. Cizmárik. *Pharmazie*, **53**, 863 (1998).
17. E.H. Ekborg-Ott, X. Wang, D.W. Armstrong. *Microchem. J.*, **62**, 26 (1999).
18. R.P.W. Scott, T.E. Beesley. *Analyst*, **124**, 713 (1999).
19. E.Tesarova, K. Zaruba, M. Flieger. *J. Chromatogr. A* **844**, 137 (1999).
20. L. Ramos, R. Bakhtiar, T. Majundas, M. Hayes, F.L.S. Tse. *Rapid Commun. Mass Spec.*, **13**, 2054 (1999).
21. R. Bakhtiar, F.L. S. Tse. *Rapid Commun. Mass Spec.*, **14**, 1128 (2000).
22. A.X. Wang, J.T. Lee, T.E. Beesley. *LCGC*, **18**, 626 (2000).
23. A. Berthod, X. Chen, J.P. Kullman, D.W. Armstrong, F. Gasparrine, I.D'Acquarica, C. Villani, A. Carotti. *Anal. Chem.*, **72**, 1767 (2000).
24. A. Karlsson, A. Aspergren. *Chromatographia*, **47**, 189 (1998).
25. T. Wang, Y.W. Chen, A. Vailaga. *J. Chromatogr.*, **902**, 345 (2000).
26. D.W. Armstrong, J.T. Lee, L.W. Chang. *Tet. Asym.* **9**, 2043 (1998).
27. D.W. Armstrong, L. He, T. Yu, J.T. Lee, Y.-S. Liu. *Tet. Asym.* **10**, 37 (1999).



## CHAPTER 3. SELECTIVE SEPARATIONS OF PEPTIDES WITH SEQUENCE DELETIONS, SINGLE AMINO ACID POLYMORPHISMS, AND/OR DIASTEREOMERS USING A TEICOPLANIN LC STATIONARY PHASE

Bo Zhang<sup>1</sup>, Renee Soukup, and Daniel W. Armstrong<sup>2</sup>

Department of Chemistry, Iowa State University, Ames IA 50011

### Abstract

Separating closely related peptides (those differing by one or two amino acids or the chirality of a single amino acid) can be challenging using reverse phase LC, ion exchange LC, or using ion-pairing agents. Also, the mobile phases that give the best separations in these modes may not be ESI-MS compatible. Forty-two peptides from eleven peptide families were separated on three macrocyclic glycopeptide stationary phases in reverse phase mode using ESI-MS compatible mobile phases. The peptide classes studied were angiotensin, bradykinin,  $\alpha$ -bag cell factor,  $\beta,\gamma$ -bag cell factor,  $\beta$ -casomorphin, dynorphin, enkephalin, leucokinin, lutinizing hormone releasing hormone, neurotensin, substance P, and vasopressin. High selectivity was observed for single amino acid substitutions (achiral and chiral) regardless of the position of the substitution in the sequence. Mobile phase optimization, its effect on peptide elution behavior, and chromatographic efficiency is also discussed. Using LC-ESI-MS, a 10 ng limit of detection was obtained, two to three orders of magnitude lower than the UV detection limit.

---

<sup>1</sup> Current address: Pfizer

<sup>2</sup> Corresponding author

Correspondence: Department of Chemistry, Iowa State University, Ames, IA 50011 Fax: 515-294-0838,  
Email: [sec4dwa@iastate.edu](mailto:sec4dwa@iastate.edu) [dwa@iastate.edu](mailto:dwa@iastate.edu)

**Keywords:** LC-ESI/MS, isocratic separations, gradient separations, enkephalins, angiotensins, bradykinins, teicoplanin, ristocetin A

## **Introduction**

The separation and analysis of peptides continues to be of paramount importance in many areas of science and technology. Some of these areas include: (a) protein sequencing, (b) analysis, quantitation, and characterization of peptide hormones, (c) synthesis of new peptide drugs, (d) pharmacokinetic and pharmacodynamic studies of pharmacologically active peptides, and (e) other fields involving the environmental, biological, and geochemical sciences.

The separation of complicated peptide mixtures is one of the more important initial steps in protein sequencing. Also, there is increasing interest in detecting single amino acid polymorphisms in proteins [1-4] which would produce the resultant peptide polymorphs after digestion with proteolytic agents. These types of protein alterations emanate from certain single nucleotide polymorphisms[5,6] and have been linked to diseases by several researchers[7-10].

Low concentrations of peptide hormones are known to elicit a large spectrum of physiological effects[11,12]. Their identification and quantification in complex biological fluids can be problematic not only because of the complicated matrices, but also due to the large number and higher concentrations of interfering substances[12]. As a consequence of these peptides' profound activity, it is not surprising that pharmaceutical scientists are synthesizing an ever-increasing number of analogues. Frequently, this involves replacing specific amino acids with other natural or more frequently, non-natural amino acid

analogues[13-17]. Non-natural amino acids can include: D-amino acids,  $\beta$ -amino acids, unusually substituted  $\alpha$ -amino acids, cyclic and bicyclic-amino acids, as well as other useful permutations [14,15]. In all cases, active potential drug candidates must undergo pharmacokinetic and pharmacodynamic studies in which they and their metabolites must be distinguished from all other naturally occurring physiological components.

Liquid chromatography (LC) is the predominant separation method used for the analysis of peptides[18-34]. It is often coupled with other separation methods and/or mass spectrometry as part of a 2-dimensional or multi-dimensional procedure[19,23,25,35]. Reverse-phase LC is the most prevalent method used because of its good resolving power, reproducibility, and ease of use [18,29,32,36]. It has become common practice to use mobile phases consisting of aqueous acetonitrile mixtures containing various ion pairing agents[26]. Ion exchange chromatography also has been used widely for the separation of peptides[24,27]. The composition of the mobile phase can be a problem if the separation is interfaced with electrospray ionization mass spectrometry (ESI-MS). Often, this is necessary to enhance both the sensitivity and selectivity of an analysis.

Given the wide variety of peptides, peptide mixtures and complex matrices in which they exist, there is a constant search for different selectivity separation approaches. For example, a porphyrin-based stationary phase was recently proposed for the separation of peptides[37]. When utilizing 2-D separations, it is usually desirable to have orthogonal separation methods. Orthogonality is more likely if the separation mechanisms are different from one another. However, the mobile phases have to be sufficiently compatible that the methods can be coupled (if using a continuous automated system).

Macrocyclic glycopeptide-based chiral (i.e., containing teicoplanin, teicoplanin aglycone, or ristocetin A) stationary phases are widely utilized for enantiomeric separations, including amino acids, dipeptides, and tripeptides[22,31]. They are known to selectively bind specific amino acids and sequences of amino acids via electrostatic, hydrogen bonding, and dipolar interactions[14,31]. It is highly likely that they also are selective for closely related peptides of any chain length. Their separation mechanism, and therefore selectivity, is significantly different from both C-18 reversed phase and ion-exchange LC. Furthermore, the mobile phases that are commonly used with teicoplanin-based stationary phases are ESI-MS compatible. The focus of this work is to evaluate the separation of a variety of closely related peptides on a teicoplanin stationary phase using isocratic elution with ESI-MS compatible mobile phases.

*Materials.* Synthetic peptides used in this study were purchased from American Peptide Company (APC) (Sunnyvale, CA) and Sigma (St. Louis, MO). The peptides, their structure, and source are listed in Table 1. Formic acid, 96%, ACS reagent grade (Sigma) was used as mobile phase additives. Acetonitrile (HPLC grade, Fisher Scientific, Pittsburgh, PA, USA) and deionized water (in-house preparation) were used to make all mobile phases. All samples were dissolved in a water/methanol (50/50) solvent mixture at 1 mg/ml concentration unless mentioned otherwise. Triethylamine (HPLC grade, Sigma.) and acetic acid (ACS grade, Fisher Scientific) were also used as mobile phase additives.

Table 1. Peptides, sequences and sources

Name	Three-letter Sequence	Single-letter sequence	Source
Leu-Enkephalin	Tyr-Gly-Gly-Phe-Leu	YGGFL	Sigma
[D-Ala <sup>2</sup> , D-Leu <sup>5</sup> ]-Enkephalin	Tyr-DAla-Gly-Phe-DLeu	Y-dA-GF-dL	APC
[Ala <sup>2</sup> ]-Leu-Enkephalin	Tyr-Ala-Gly-Phe-Leu	YAGFL	APC
Met-Enkephalin	Tyr-Gly-Gly-Phe-Met	YGGFM	Sigma
Met-Enkephalin [D-Ala <sup>2</sup> ]	Tyr-DAla-Gly-Phe-Met	Y-dA-GFM	APC
[D-Ala <sup>2</sup> , Leu <sup>5</sup> ]-Enkephalin	Tyr-DAla-Gly-Phe-Leu	Y-dA-GFL	APC
[DAla <sup>2,4</sup> , Tyr <sup>5</sup> ] b-Casomorphin (1-5), amide, bovine	Tyr-DAla-Phe-D-Ala-Tyr-NH <sub>2</sub>	Y-dA-F-dA-Y-NH <sub>2</sub>	APC
[DAla <sup>2</sup> , DPro <sup>4</sup> , Tyr <sup>5</sup> ] b-Casomorphin (1-5), amide	Tyr-DAla-Phe-DPro-Tyr-NH <sub>2</sub>	Y-dA-F-dP-Y-NH <sub>2</sub>	APC
[DAla <sup>2</sup> , Hyp <sup>4</sup> , Tyr <sup>5</sup> ] b-Casomorphin (1-5), amide	Tyr-DAla-Phe-Hyp-Tyr-NH <sub>2</sub>	Y-dA-F-Hyp-Y-NH <sub>2</sub>	APC
β-Bag Cell Factor	Arg-Leu-Arg-Phe-His	RLRFH	APC
γ-Bag Cell Factor	Arg-Leu-Arg-Phe-Asp	RLRFD	APC
α-Bag Cell Peptide (1-7)	Ala-Pro-Arg-Leu-Arg-Phe-Tyr	APRLRFY	APC
α-Bag Cell Peptide (1-8)	Ala-Pro-Arg-Leu-Arg-Phe-Tyr-Ser	APRLRFYS	APC
α-Bag Cell Peptide (1-9)	Ala-Pro-Arg-Leu-Arg-Phe-Tyr-Ser-Leu	APRLRFYSL	APC
Leucokinin I	Asp-Pro-Ala-Phe-Asn-Ser-Trp-Gly-NH <sub>2</sub>	DPAFNSWG-NH <sub>2</sub>	APC
Leucokinin II	Asp-Pro-Gly-Phe-Ser-Ser-Trp-Gly-NH <sub>2</sub>	DPGFSSWG-NH <sub>2</sub>	APC
Leucokinin VII	Asp-Pro-Ala-Phe-Ser-Ser-Trp-Gly-NH <sub>2</sub>	DPAFSSWG-NH <sub>2</sub>	APC
[Sar <sup>1</sup> , Thr <sup>8</sup> ]-Angiotensin II	Sar-Arg-Val-Tyr-Ile-His-Pro-Thr	Sar-RVYIHPT	Sigma
Angiotensin II human	Asp-Arg-Val-Tyr-Ile-His-Pro-Phe	DRVYIHPF	Sigma
[Val <sup>5</sup> ]-Angiotensin II	Asp-Arg-Val-Tyr-Val-His-Pro-Phe	DRVYVHPF	Sigma
Angiotensin II antipeptide	Glu-Gly-Val-Tyr-Val-His-Pro-Val	EGVYVHPF	Sigma
[Sar <sup>1</sup> ]-Angiotensin II	Sar-Arg-Val-Tyr-Ile-His-Pro-Phe	Sar-RVYIHPF	Sigma
Bradykinin	Arg-Pro-Pro-Gly-Phe-Ser-Pro-Phe-Arg	RPPGFSPFR	Sigma
des-Pro <sup>2</sup> -Bradykinin	Arg-Pro-Gly-Phe-Ser-Pro-Phe-Arg	RPGFSPFR	Sigma
Bradykinin Fragment 2-7	Pro-Pro-Gly-Phe-Ser-Pro	PPGFSP	Sigma
Bradykinin Fragment 2-9	Pro-Pro-Gly-Phe-Ser-Pro-Phe-Arg	PPGFSPFR	Sigma
[Lys <sup>8</sup> ] Vasopressin	Cys-Tyr-Phe-Gln-Asn-Cys-Pro-Lys-Gly-NH <sub>2</sub>	CYFQNCPKG-NH <sub>2</sub>	APC
[Arg <sup>8</sup> ] Vasopressin /AVP	Cys-Tyr-Phe-Gln-Asn-Cys-Pro-Arg-Gly-NH <sub>2</sub>	CYFQACPRG-NH <sub>2</sub>	APC

Table 1. (continued)

Dynorphin A (1-10), porcine	Tyr-Gly-Gly-Phe-Leu-Arg-Arg-Ile-Arg-Pro	YGGFLRRIRP	APC
Dynorphin A (1-10), amide, porcine	Tyr-Gly-Gly-Phe-Leu-Arg-Arg-Ile-Arg-Pro-NH <sub>2</sub>	TGGFLRRIRP-NH <sub>2</sub>	APC
[D-Ala <sup>6</sup> ]-LH-RH	pGlu-His-Trp-Ser-Tyr-D-Ala-Leu-Arg-Pro-Gly-NH <sub>2</sub>	pEHWSY-dA-LRPG-NH <sub>2</sub>	Sigma
[des-pGlu <sup>1</sup> ]-LH-RH	His-Trp-Ser-Tyr-Gly-Leu-Arg-Pro-Gly-NH <sub>2</sub>	HWSYGLRPG-NH <sub>2</sub>	Sigma
[D-Lys <sup>6</sup> ]-LH-RH	pGlu-His-Trp-Ser-Tyr-D-Lys-Leu-Arg-Pro-Gly-NH <sub>2</sub>	pEHWSY-dK-LRPG-NH <sub>2</sub>	Sigma
[D-Phe <sup>2</sup> ,D-Ala <sup>6</sup> ]-LH-RH	pGlu-D-Phe-Trp-Ser-Tyr-D-Ala-Leu-Arg-Pro-Gly-NH <sub>2</sub>	Pe-dF-WSY-dA-LRPG-NH <sub>2</sub>	Sigma
Neurotensin	pGlu-Leu-Tyr-Glu-Asn-Lys-Pro-Arg-Arg-Pro-Tyr-Ile-Leu	pELYENKPRRPYIL	Sigma
[Phe <sup>11</sup> ]-Neurotensin	pGlu-Leu-Tyr-Glu-Asn-Lys-Pro-Arg-Arg-Pro-Phe-Ile-Leu	pELYENKPRRPFIL	Sigma
[DTrp <sup>11</sup> ] Neurotensin	Glp-Leu-Tyr-Glu-Asn-Lys-Pro-Arg-Arg-Pro-DTrp-Ile-Leu	pELYENKPRRP-dW-IL	APC
[DTyr <sup>11</sup> ] Neurotensin	Glp-Leu-Tyr-Glu-Asn-Lys-Pro-Arg-Arg-Pro-DTyr-Ile-Leu	pELYENKPRRP-dY-IL	APC
[Gln <sup>4</sup> ] Neurotensin	Glp-Leu-Tyr-Gln-Asn-Lys-Pro-Arg-Arg-Pro-Tyr-Ile-Leu	pELYQNKPRRPYIL	APC
Neurotensin, guinea pig	Glp-Leu-Tyr-Glu-Asn-Lys-Ser-Arg-Arg-Pro-Tyr-Ile-Leu	pELYENKSRRPYIL	APC
[DPro <sup>10</sup> ] Dynorphin A (1-11), porcine	Tyr-Gly-Gly-Phe-Leu-Arg-Arg-Ile-Arg-DPro-Lys	YGGFLRRIR-dP-K	APC
Dynorphin A (1-11), porcine	Tyr-Gly-Gly-Phe-Leu-Arg-Arg-Ile-Arg-Pro-Lys	YGGFLRRIRPK	APC
Dynorphin A (1-13), porcine	Tyr-Gly-Gly-Phe-Leu-Arg-Arg-Ile-Arg-Pro-Lys-Leu-Lys	YGGFLRRIRPKLK	APC
[DArg <sup>6</sup> ] Dynorphin A (1-13), porcine	Tyr-Gly-Gly-Phe-Leu-DArg-Arg-Ile-Arg-Pro-Lys-Leu-Lys	YGGFL-dR-RIRPKLK	APC
[Nor <sup>8</sup> ] Substance P	DPro-Gln-Gln-DTrp-Phe-DTrp-Leu-Nor-NH <sub>2</sub>	dP-QQ-dW-F-dW-LN-NH <sub>2</sub>	APC
Substance P	DPro-Gln-Gln-DTrp-Phe-DTrp-Leu-Met-NH <sub>2</sub>	dP-QQ-dW-F-dW-LM-NH <sub>2</sub>	APC

*Instrument.* The chromatographic methods were developed on a HP (Palo Alto, CA, USA) 1050 HPLC system, including: 1 auto sampler, 1 quaternary pump, and 1 VWD detector. All separations were carried out with analytical columns from Advanced Separation Technologies (ASTEC, Whippany, NJ, USA) at room temperature. The columns used were Chirobiotic T (250 x 4.6 mm), Chirobiotic R (250 x 4.6 mm), Chirobiotic TAG (250 x 4.6 mm). LC/MS analyses were carried out on a Thermo Finnigan (San Jose, CA, USA) Surveyor LC system coupled with Thermo Finnigan LCQ Advantage API ion-trap mass spectrometer with ESI source. Ultra-high purity helium gas (Linweld, Lincoln, NE, USA) was used as dampening gas. Praxair (Danbury, CT, USA) Nitrogen was used as sheath gas and auxiliary gases.

## Methods

All HPLC methods are listed in Table 2. Depending on mobile phase conditions, UV/Vis detection was performed at wavelengths of 210 nm, 232 nm, or 254 nm. ESI conditions were set to the following: sheath gas = 50 arbitrary units, auxiliary gas = 40 arbitrary units, source voltage = 4.55 kV, capillary voltage = 30.6 V, tube lens offset = -15.0 V, and capillary temperature = 272 °C. LC/MS experiments were carried out using flow rates of 1.0 mL/min, unless noted otherwise.

## Results and Discussion

### *Peptide separations*

Macrocyclic glycopeptide CSPs exhibited excellent selectivity in separating closely related peptides. Figure 1 shows the baseline resolution of six enkephalin peptides on the

Chirobiotic T (teicoplanin) column in single isocratic run. The enkephalin peptides are closely related structurally, differing from one another by only one amino acid or the chirality of an single amino acid. In additional, retention times can be reduced substantially, if desired, by utilizing gradient elution. Currie et al. had some success in resolving enkephalin peptides by using a phenyl bonded column[38]. But no baseline separation was achieved when four or more enkephalin peptides were present in the mixture. Underberg, et al. recently coupled size exclusion chromatography (SEC) and RP-LC to separate large proteins and Enkephalin peptides[39]. Although separation was achieved, the system complexity and low chromatographic quality made the separation less desirable. In addition to the good selectivity observed in Figure 1, the mobile phase is ESI-MS compatible (as will be shown and discussed for subsequent separations).

Excellent separations were commonly observed for most of the peptides listed in Table 2. Within each family (listed in Table 2), the individual peptides are listed in the order of their retention at the elution conditions specified. The selectivity ( $\alpha$ ) and resolution ( $R_s$ ) values are reported for adjacent peptide peaks within each family. These values were calculated at optimized isocratic elution conditions for the separation of the entire peptide family. Other elution conditions can be found to further resolve any single pair of peptides within the family, if desired. Table 3 indicates the macrocyclic glycopeptide column that produced the most effectie separations for each class (family)of peptides. The Chirobiotic T column produced the best separations for the largest numbers of families, but all three columns were needed to separate the all of the families.



Table 2. Selectivity ( $\alpha$ ) and Resolution ( $R_s$ ) for Peptides on T, TAG and R stationary phases.

Peptides	Columns								
	Chirobiotic T			Chirobiotic TAG			Chirobiotic R		
	MP <sup>b</sup>	$\alpha^a$	$R_s^a$	MP <sup>b</sup>	$\alpha^a$	$R_s^a$	MP <sup>b</sup>	$\alpha^a$	$R_s^a$
<b>Enkephalins</b>									
Y-dA-GF-dL	B			A			C		
Y-dA-GFM	1 mL/min	1.09	1.75	2 mL/min	1.14	2.31	1 mL/min	1.24	2.71
YGGFM		1.21	4.07		1.2	3.29		1.18	2.04
Y-dA-GFL		1.32	5.94		1.3	4.48		1.13	1.39
YGGFL		1.26	5		1.24	3.56		1.06	0.06
YAGFL		1.18	3.72		1	0		1.09	0.96
<b><math>\beta</math> <math>\gamma</math> Bag Cell Factors</b>									
RLRFH	F						E		
RLRFD	2 mL/min	2.41	11.58				2 mL/min	2.96	2.58
<b><math>\delta</math>-Casomorphins</b>									
Y-dA-F-dA-Y-NH2	H						I		
Y-dA-F-dP-Y-NH2	1 mL/min	1.11	2.05				1 mL/min	1.19	0.64
Y-dA-F-Hyp-Y-NH2		1.32	5.44					1.95	2.56
<b><math>\alpha</math> Bag Cell Factors 7,8,9</b>									
APLRFY				O			L		
APLRFYS				1.5 mL/min	1.32	2.29	1 mL/min	1.15	1.3
APLRFYSL					1.29	2.05		1.25	1.72
<b>Leucokins</b>									
DPAFSSWG-NH2	C						C		
DPGFSSWG-NH2	1.2 mL/min	1.07	1.54				1 mL/min	1.11	0.82
DPAFNSWG-NH2		1.12	2.81					1.28	1.74
<b>Angiotensins</b>									
EGVYVHPE	P						G		
DRVYIHPE	0.5 mL/min	1.93	13.3				2 mL/min	1.52	3.26
N-methyl-GRVYIHPT		1.06	1.25					1.45	2.93
N-methyl-GRVYIHPE		1.09	1.74					1.46	2.94
DRVYVHPE		1.07	1.39					1	
<b>Substance P</b>									
dP-QQ-dW-F-dW-LN-NH2	1.0 mL/min						1 mL/min	5.00	1.33
dP-QQ-dW-F-dW-LM-NH2		5.93	21.2						
<b>Bradykinins</b>									
PPGFSPFR	M						K		
PPGFSPFR	1 mL/min	2.2	15.12				1.2 mL/min	1.8	3.86
RPGFSPFR		2.37	15.39					2.16	2.16
RPPGFSPFR		1.1	1.82					1.31	1.31

a.)  $\alpha = k'_2/k'_1$ ,  $R_s = (2 * (t_2 - t_1)) / (w_1 + w_2)$

b.) Mobile Phases: (A) ACN/Water 65/35 (B) ACN/Water 75/25 (C) ACN/Water 85/15 (D) ACN/ 5 mM Ammonium Formate aqueous solution pH 3 55/45 (E) ACN/5mM Ammonium Formate aqueous solution pH 3 60/40 (F) ACN/25 mM Ammonium Formate, pH3.0 30/70 (G) ACN/5mM Ammonium Formate aqueous solution pH 3 65/35 (H) ACN/16 mM Ammonium Formate pH as is 75/25 (I) ACN/16 mM Ammonium Formate pH as is 90/10 (J) ACN/20mM Ammonium Formate pH as is 20/80 (K) ACN/32mM Ammonium Formate pH as is 50/50 (L) ACN/40 mM Ammonium Formate pH as is 60/40 (M) ACN/0.06% Formic acid aqueous solution 35/65 (N) ACN/0.1% Formic acid aqueous solution 25/75 (O) ACN/0.1% Formic acid aqueous solution 30/70 (P) ACN/0.1% Formic acid aqueous solution 35/65 (Q) ACN/0.1% Formic acid aqueous solution 40/60 (R) ACN/0.75% Triethylamine pH 2.8 40/60 (S) ACN/ 1% Triethylamine pH 2.8 20/80

Table 2. (continued)

	Columns								
	Chirobiotic T			Chirobiotic TAG			Chirobiotic R		
<i>Vasopressins</i>									
CYFQNCPKG-NH2	O			Q			J		
CYFQACPRG-NH2	1 mL/min			1 mL/min	1.25	2.31	1 mL/min	1.16	1.8
<i>Dynorphins</i>									
YGGFLRR									
IRP	Q								
TGGFLRRIRP-NH2	1.5 mL/min	1.26	2.3						
<i>Luteinizing Hormone Releasing Hormone</i>									
Pc-dF-WSY-dA-LRPG-NH2	P						G		
pEHWSY-dA-LRPG-NH2	1 mL/min	1.38	5.16				1 mL/min	2.34	7.68
pEHWSY-dK-LRPG-NH2		1.71	8.56					2.14	3.48
HWSYGLRPG-NH2		1.2	2.92					1.3	1.32
<i>Neurotensins</i>									
pELYENKPRRP-dW-IL	N								
pELYENKPRRP-dY-IL	1 mL/min	1.26	1.63				G	1.15	1.24
pELYENKPRRPYIL		1.08	0.83				1 mL/min	1.28	2.04
pELYENKPRRPFIL		1.07	0.82					1.22	1.75
pELYQNKPRRPYIL		1.09	0.76					1.25	1.97
pELYENKSRRPYIL		0	0					1.48	1.69
<i>Dynorphin 1-11</i>									
YGGFLRRIR-dP-K	R								
YGGFLRRIRPK	0.8 mL/min	1.12	1.53						
<i>Dynorphin 1-13</i>									
YGGFL-dR-RIRPKL.K	S								
YGGFLRRIRPK	1 mL/min	1.19	1.95						

### *Separation of Peptides containing single amino acid polymorphism (SAAP)*

As demonstrated in Figure 1, the enkephalins were easily baseline separated from each other. Among these separations, enkephalin peaks 2 and 4, enkephalin peaks 3 and 5, enkephalin peaks 5 and 6 are different from each other only by a single amino acid. A particular separation of note is the SAAP represented in peaks 5 and 6. The glycine in position 2 of one peptide is replaced with an alanine. This difference in the side chains is one

of the more subtle substitutions among native amino acids, yet it is easily separated. enkephalin peaks 1 and 4, and enkephalins peak 4 and 6 differ from each other only by the chirality of a single amino acid, making them epimers of one another. Interestingly, these single amino acid chirality polymorphism (SAACP) peptides weren't eluted next to each other. At least one other peptide eluted between the epimers. The epimeric position in the peptide chain might play a critical role in determining if the separation is substantial enough to allow another peptide to elute between the epimers, as this behavior was not always observed.

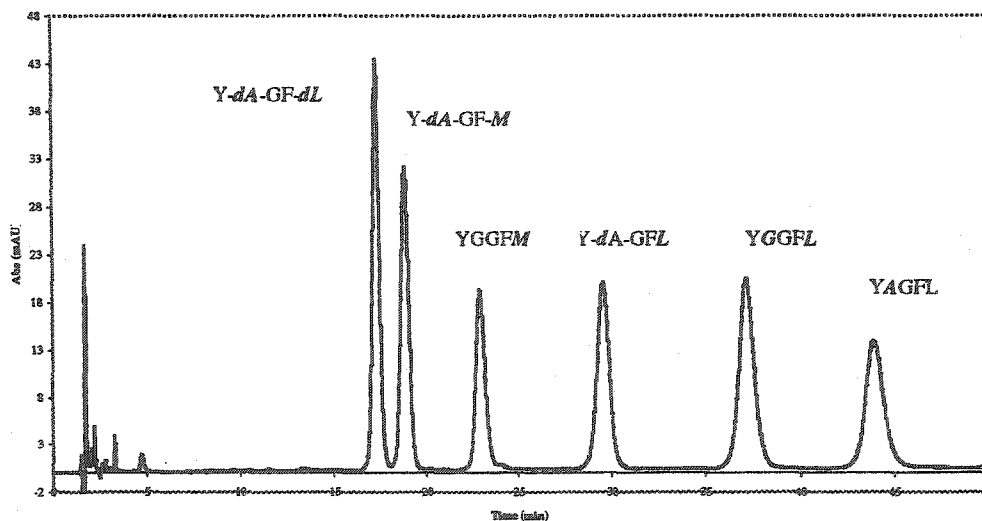
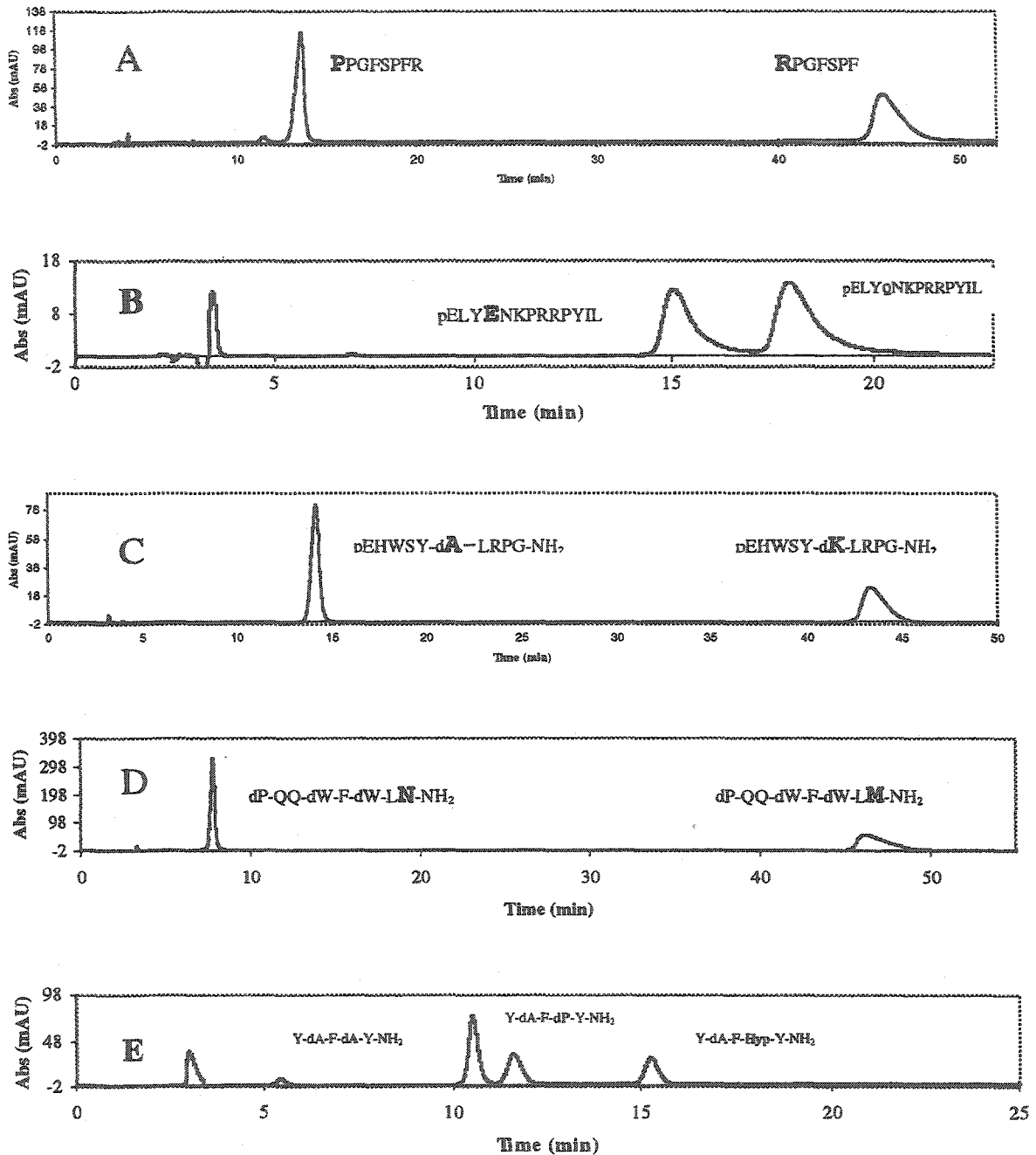


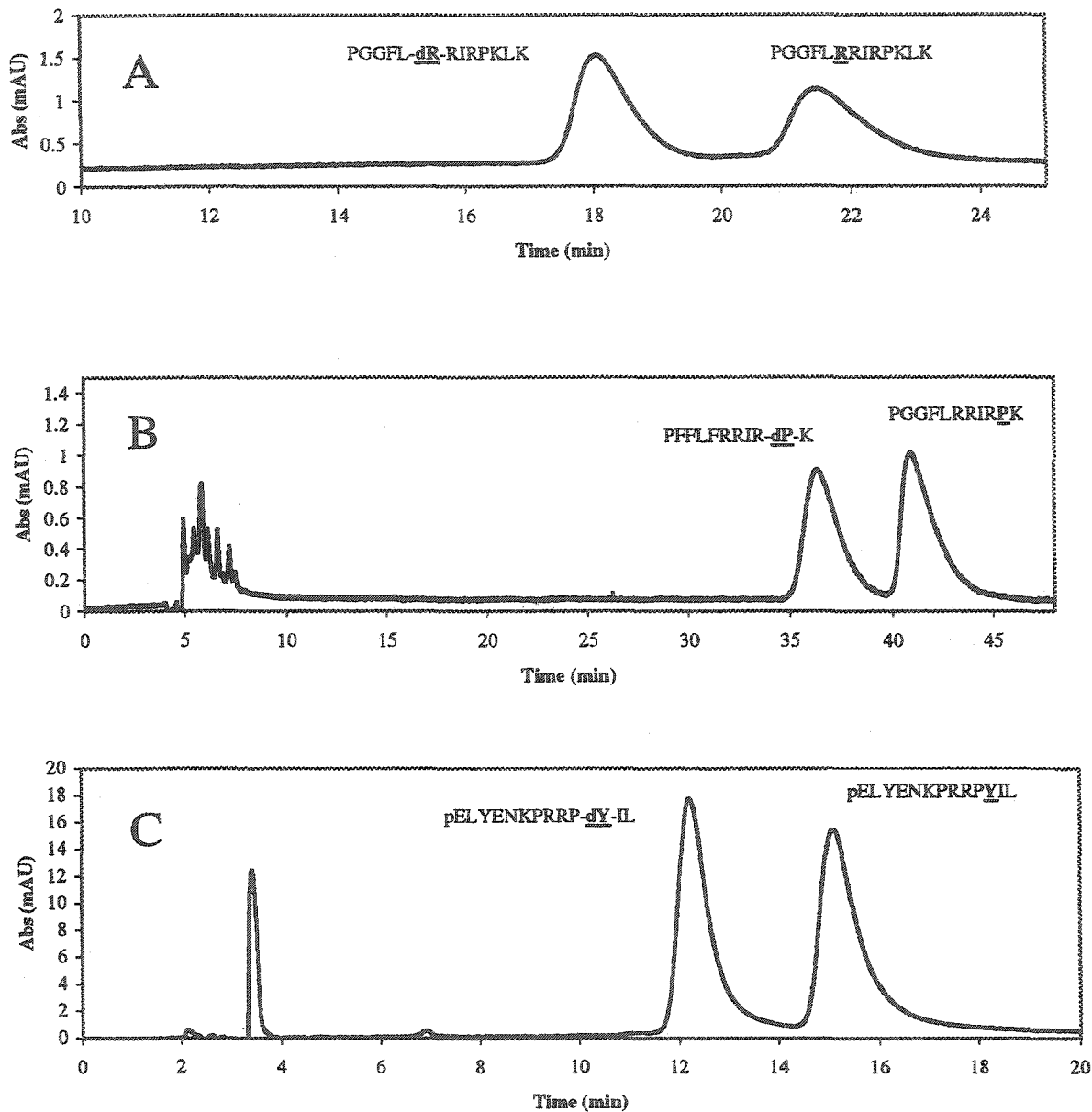
Figure 1. Separation of six enkephalin peptides on Chirobiotic T column. Single amino acid polymorphisms (SAAP) occur in (a) peaks 2 and 4, (b) peaks 3 and 5, and (c) peaks 5 and 6. Examples of chiral amino acid polymorphisms are (a) peaks 1 and 4 and (b) peaks 4 and 6. Chromatographic conditions are given in table 2.

Figure 2 shows several separations of peptides with SAAP. Separation is achieved regardless of whether the amino acid substitution occurs at the N- terminus, middle, or C-terminus of the peptide chain. In each related sequence, the amino acid that is different is highlighted for easier comparison (Figure 2, Table 2). In general, the separation was easier

to achieve if the polymorphism occurred at or near the end of peptide chain. This is because functional groups on both ends provide stronger interaction with the stationary phase [31]. It is important to note that these separations were obtained under optimized elution conditions for the entire family of peptides. In the cases where a neutral amino acid is replaced with a positively charged amino acid (Figure 2A and 2C), there is a tremendous difference in the retention of the peptides. This is largely due to the additional interaction of cationic side chains with the stationary phase. However, differences in electrostatic interactions are not solely responsible for the ultra-high selectivities. For example, the substitution of methionine for norleucine (Figure 2D) also produces a tremendous change in the retention behavior of these peptides. Figure 3 shows the separation of peptide epimers (i.e. where the single amino acid polymorphism is due to the opposite chirality of a single amino acid). In these cases, peptides with the chiral SAAP in the middle of the peptide chain were as easy to separate as those with more terminal groups. However, epimers in which the chiral SAAP is  $\alpha$  or  $\beta$  to the C-terminal end (Figure 1) appear to produce the most facile separations of this class of diastereomers. Interestingly, the epimer containing the D-amino acid always eluted before the other epimer, regardless of its position in the peptide chain (Figure 1 and 3). It should be noted that this elution sequence is opposite to that observed for monomer native amino acids and dipeptides [31].



**Figure 2.** Chromatograms showing the effect of the location of a SAAP within the peptide on the separation of the polymorphs. The polymorphism occurs at the (A) N-terminus (Bradykinin family), (B, E) position 4 (Neurotensin,  $\beta$ -Casomorphin families), (C) position 6 (Lutenizing Hormone Releasing Hormone family) or the (D) C-terminus (Substance P family) of the peptide. Chromatograms A, C, D, E were generated on a Chirobiotic T column and Chromatogram B was generated on a Chirobiotic R column. All chromatographic conditions same as in Table 1.



**Figure 3.** Chromatograms showing the effect of the location of a chiral SAAP within the peptide on the separation of the polymorphs. The polymorphism occurs in (A) position 6 (Dynorphin 1-11 family), (B) position 6 (Dynorphin 1-13 family) or (C) position 11 (Neurotensin family). Chromatograms A and B were produced on a Chirobiotic T column; Chromatogram C was produced on a Chirobiotic R column. All chromatographic conditions the same as in Table 2.

### *Optimization of Peptide Separations on Chirobiotic Stationary Phases*

As with most separations of charged analytes in the reverse phase mode, the percentage and type of organic modifier along with the pH of the mobile phase, must be optimized in order to produce the best separation. Since the macrocyclic glycopeptide stationary phases also have ionic sites, the ionic strength of the mobile phase must also be considered.

#### Organic Modifier Content and Retention Behavior

In separating small molecules in the reversed phase mode, most macrocyclic glycopeptide stationary phases have shown the highest selectivity when methanol was used as the organic modifier. While this also was true for the peptides examined here, methanol often produced broad peaks and inefficient separations. Efficiency was greatly improved when acetonitrile was used as the organic modifier. Acetonitrile was used in all the mobile phases reported here, as the increase in efficiency more than compensated for the loss in selectivity.

Regardless of organic modifier type, plots of mobile phase composition (i.e., percent organic modifier) versus retention produced U-shaped retention curve behavior on all macrocyclic glycopeptide stationary phases. Figure 4 shows the elution behavior for two Vasopressin peptides on a Chirobiotic TAG stationary phase. The peptides are more strongly retained under high organic content and high aqueous content mobile phases. The strongest eluting mobile phase was generally around half organic and half aqueous content, although the sequence of the peptide determines the exact location (composition) of the minimum for any retention versus composition curve. Similar U-shape retention behavior of peptides and proteins was commonly observed on alkyl bonded stationary phases [40-48],

despite their differences in chemistry from macrocyclic glycopeptide stationary phases. Moritz et al. indicated that peptide retention, at high organic modifier concentration, was more like normal phase chromatography (polar stationary phase), which suggests that residual silanol groups also contribute greatly in retention[42]. Horvath and co-workers proposed dual mechanisms, in which the combination of solvophobic and silanophilic interaction was thought to be the reason for retention inversion[48]. Early on, Armstrong et al. pointed out that the real reason for the inverse retention behavior at high organic modifier concentration (for many proteins, peptides, and even amino acids) was from the changes in their solubility as the organic concentration in the mobile phase is increased [40,41]. Under high aqueous mobile phase conditions the classic reverse phase mechanism (i.e., hydrophobic association) governs retention, where increased organic modifier amounts decrease retention. Under high organic mobile phase content, peptides become much less soluble in the mobile phase, which means longer retention times. The point of minimum retention (Figure 2) can be approximated by coupling the reversed phase retention curve and the solubility curve for any peptide of interest. In some cases, other specific interactions (electrostatic, etc.) can affect the exact location of the retention minimum. The U-shaped elution curve behavior also indicates the possibility to carry out an inverse gradient on this class of stationary phases [40]. Thus, more choices in method development are available. Most mobile phases in this work use higher organic modifier concentrations due to the increased efficiency observed with such mobile phases.



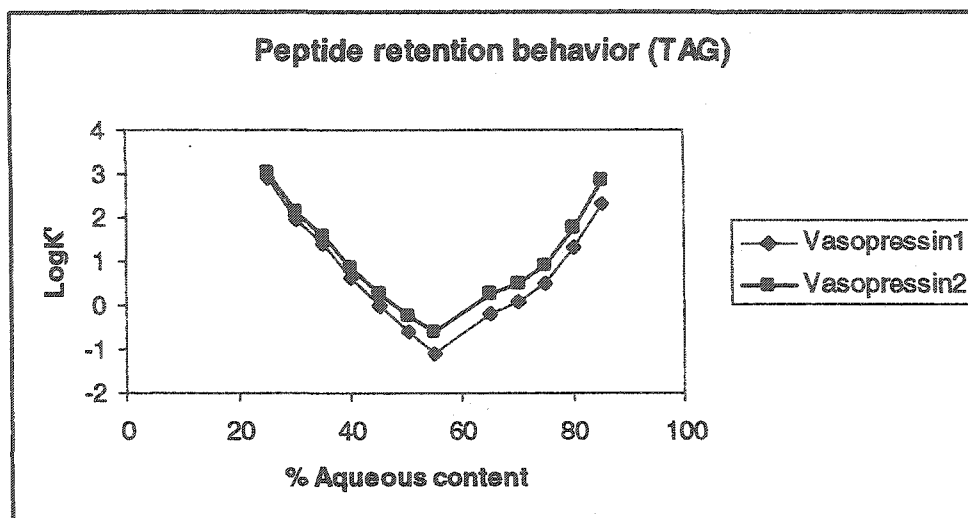


Figure 4. Retention of Vasopressin peptides on the Chirobiotic TAG stationary phase. Increased retention at high organic modifier content is observed due to lower peptide solubility in the mobile phase. Chromatographic conditions: Chirobiotic TAG 250 x 4.6mm column at a flow rate of 1mL/min with UV detection at 210 nm. Aqueous solution included 0.1% formic acid.

#### Mobile phase pH

The overall charge on a peptide is determined by the amino acids in the peptide and is a consideration in determining the optimized mobile phase. Under the operating pH range of the macrocyclic glycopeptide stationary phases (pH 2.8-7.5), peptides with basic side chain groups are generally protonated while peptides with acidic side chain groups are deprotonated. The additional positively charged side chains allow for increased interaction of the peptide with the stationary phase through its anionic sites. Thus, cationic peptides can be strongly retained [31]. Adding ammonium salts or acidifying the mobile phase appears to provide competing ions for the anionic sites or protonate them, respectively, thereby decreasing the retention of positively charged peptides. However, for neutral and anionic peptides, the ammonium salt or acid can overwhelm the interaction of the peptide with the stationary phase leading to insufficient retention. Some neutral peptides (e.g. enkephalins)

elute with the void volume if salt or acid is added to the mobile phase. Additionally, the specific structure of the stationary phases must be considered as well. For the Chirobiotic T and TAG columns, the mobile phase additive formic acid was required to elute many of the peptides listed in Table 2. However, when the same mobile phase conditions used for separations on the Chirobiotic T or TAG columns are used on the Chirobiotic R column, the peptides elute with the void volume (data not shown). This change in behavior is due to the presence (or absence) carboxylic acid sites on the stationary phase. Teicoplanin (Chirobiotic T) and the teicoplanin aglycone (Chirobiotic TAG) have a free carboxylic acid group while the corresponding acid site on the ristocetin (Chirobiotic R) has been esterified.

To illustrate the effect of mobile phase additives on retention, peak shape, and resolution, different amounts ammonium formate were added to the mobile while maintaining a constant pH and acetonitrile content. The Bradykinin peptides were chosen because this family of peptides contains both neutral and cationic side chains. Peptides with cationic side chains contain up to two arginine residues. Figure 5 shows chromatograms generated using mobile phases containing different ammonium formate concentrations of 2mM, 5mM, 15mM, and 25 mM. At 2mM ammonium formate, RPGFSPFR and RPPGFSPFR took over 100 minutes to elute (data not shown). Only the first twenty minutes of the chromatogram is shown in order to compare the peak shape for the two peptides that did elute. The basic arginine group in PPGFSPFR produces much more pronounced tailing at this concentration relative to the PPGFSP peptide, which contains no amino acids with cationic side chains. Increasing the ammonium formate concentration to 5mM drastically shortens the retention times of the peptides with two arginines residues. However, the more

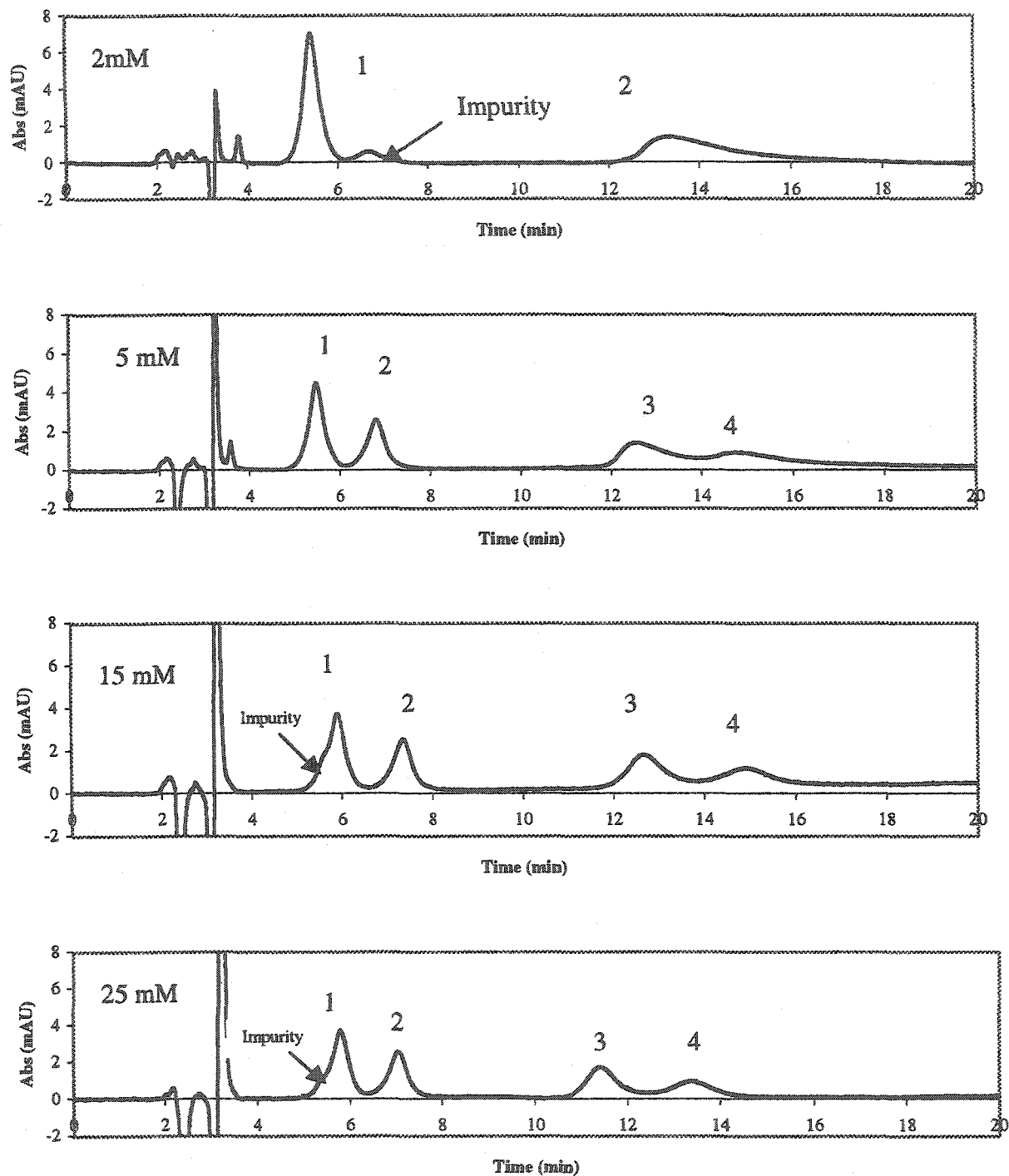


**Figure 5.** The four chromatograms show the effect of ionic strength on the elution of charged peptides. Peptides are from the Bradykinin family and the sequence is as follows: (1) PPGFSP (2) PPGFSPFR (3) RPPGFSPFR (4) RPPGFSPFR. Chromatographic conditions: Chirobiotic R column, 60% ACN/ 40% Ammonium Formate buffer pH 3, 1.0mL/min.

basic peptides still exhibit broad peaks with significant tailing. Raising the ammonium formate concentration to 15 and 25mM continues to shorten the retention times of the basic peptides while leaving the retention of PPGFSP relatively constant. Greater efficiency is achieved at 15 and 25 mM compared to 5mM, though changes tend to be less pronounced. It is expected that higher concentrations of ammonium formate could further enhance peak shape of the more basic peptides. However, the most MS-compatible mobile phase would utilize the lowest salt concentration to give the desired detection sensitivity (as discussed in the following section).

#### *Electrospray-Mass Spectrometry Detection*

Many previous LC methods, developed to separate peptides, used alkyl bonded phases with ion pairing agents such as: trifluoroethylammonium phosphate[49], trifluoroacetic acid (TFA), trialkyl ammonium phosphate (TAAP)[50], or heptafluorobutyric acid (HFBA)[51,52]. By using these agents in mobile phases under appropriate pH conditions, charged analytes like peptides would form pairs of ions. Instead of eluting in the dead volume, peptides could be retained and separated due to their different hydrophobic interactions with the stationary phase. With the increasing popularity of electrospray ionization mass spectrometry coupled to HPLC, alternatives to the ion pair approach have been sought because of the adverse effects of ion pair reagents on ESI ionization efficiency[53,54]. In this study, all but two of the mobile phases developed were MS compatible. Triethylamine was added to the mobile phase in order to separate the epimers of the Dynorphin family. The large number of basic amino acids present in this family of

peptides caused them to interact very strongly with the stationary phase. Triethylamine at pH 2.8 provides stronger competition for the stationary phase than other mobile phase additives.

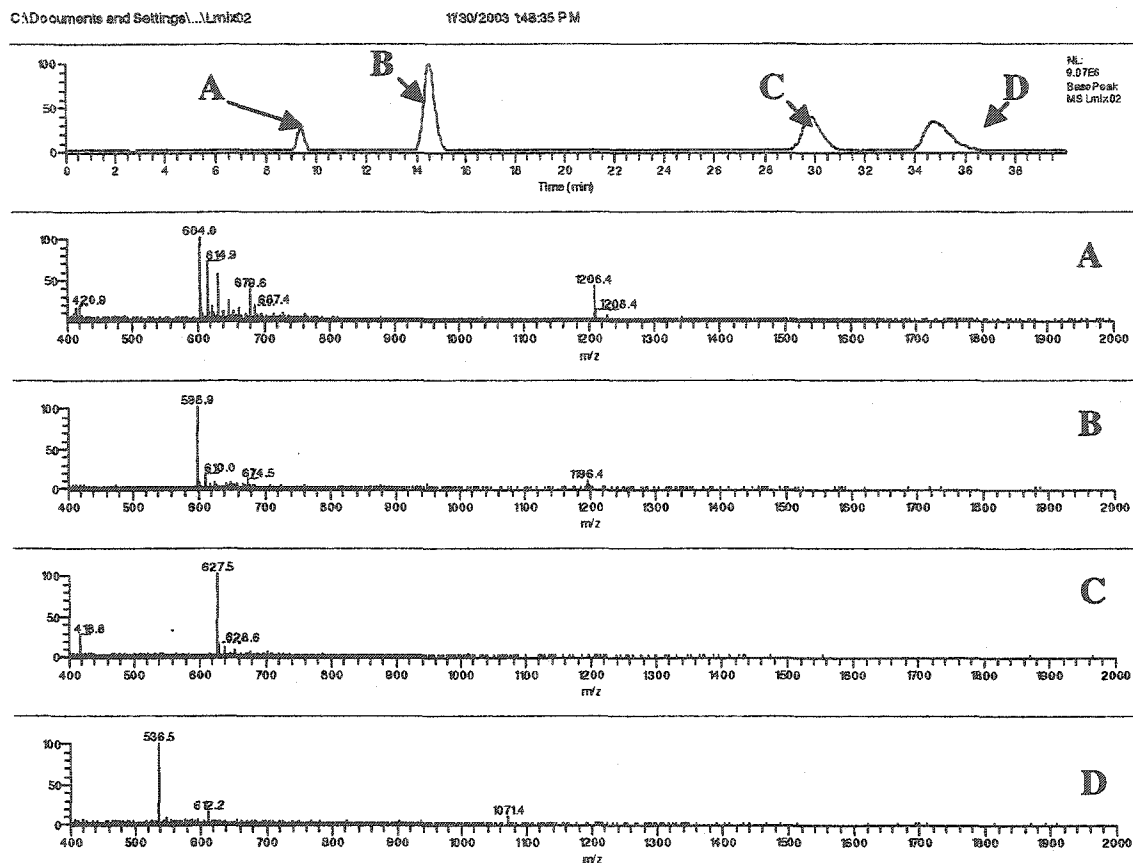
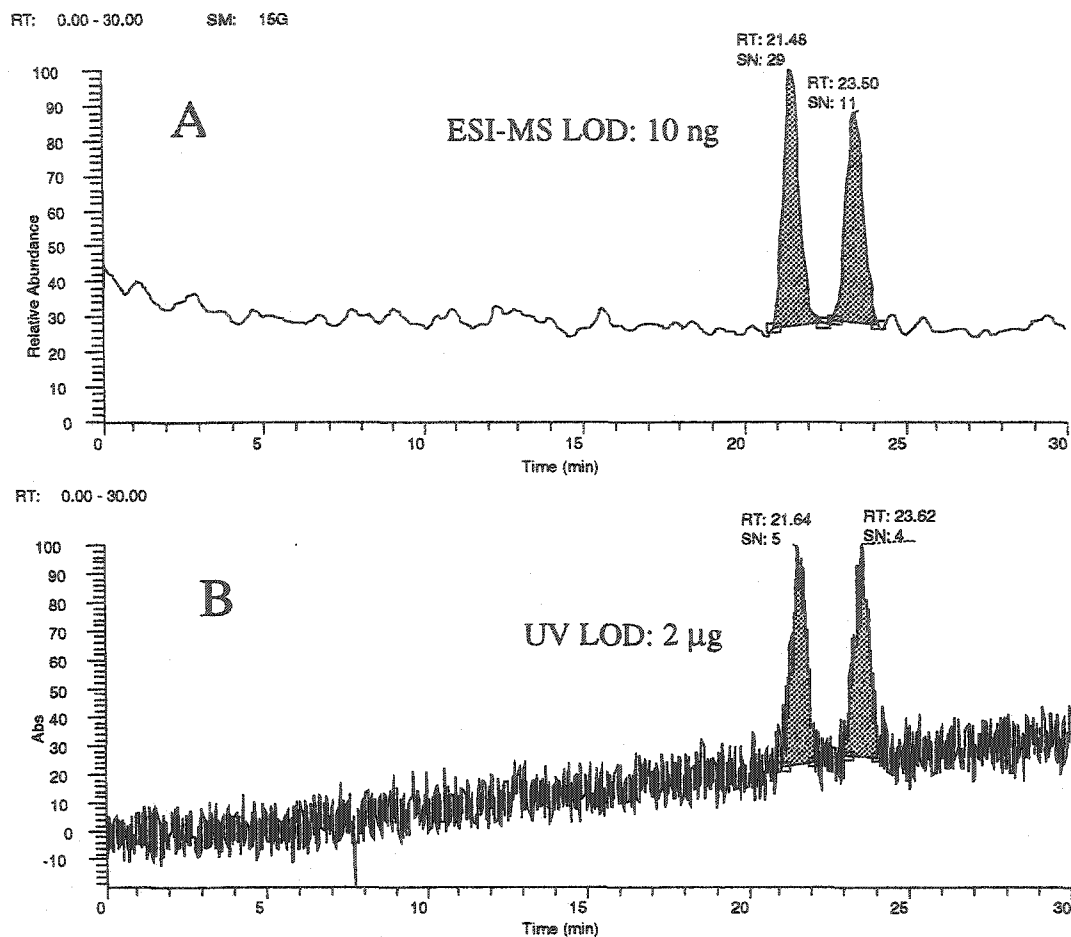


Figure 6. LC/ESI/MS of the Luteinizing Hormone Releasing Hormone family. Panel A is total ion chromatogram (TIC). Panel B, C, D, E are the mass spectra of each peak in panel A. HPLC conditions: Antibiotic T 250x4.6 mm column; mobile phase composition: 60% 0.1% Formic acid, 40% Acetonitrile. Flow rate 1 ml/min.

Figure 6 shows an example separation of luteinizing hormone releasing hormone peptides using ESI/MS detection. The isocratic HPLC method is simple and ESI/MS compatible. From the mass spectra, the peaks can be easily identified according to their molecular weight. The most abundant ion was usually the  $[M+2H]^{2+}$  species, although

sodium adduct products also were observed. This behavior is consistent with ESI spectra of peptides reported elsewhere [55].



**Figure 7.** The limits of detection for the Vasopressin peptides were found for both (A) ESI/MS (SIM mode) and (B) UV (210nm) detection. Injection volumes were identical for both panels. HPLC conditions: Antibiotic TAG 250x4.6mm, using a mobile phase composition of 60% 0.1% formic acid aqueous solution, 40% Acetonitrile at 0.5 ml/min.

In the recent literature, Desai et. al. reported the detection limits of amino acids in nanograms and sub nanograms level by atmospheric pressure chemical ionization mass spectrometry (APCI/MS)[53]. In this study, APCI/MS gave the best sensitivity for small

molecules under 200 Da and similar sensitivity to ESI/MS for molecules between 200 and 300 Da. Above 300 Da, sensitivity increased for ESI/MS compared to APCI/MS. Figure 7 compares the detection limit of ESI/MS and UV. A 10ng peptide detection limit was easily achieved by ESI/MS in this study, consistent with the level for single amino acids in Desai's report. This 10 ng detection limit is between two and three orders of magnitude lower than the detection limit obtained using UV detection at 210 nm under identical conditions.

Figure 8 shows that there is good detection linearity over wide range of peptide concentrations. The methods developed in this study provide not only sensitive detection but also respectable detection linearity. This sensitive detection with a linear response is necessary for modern peptide assays.

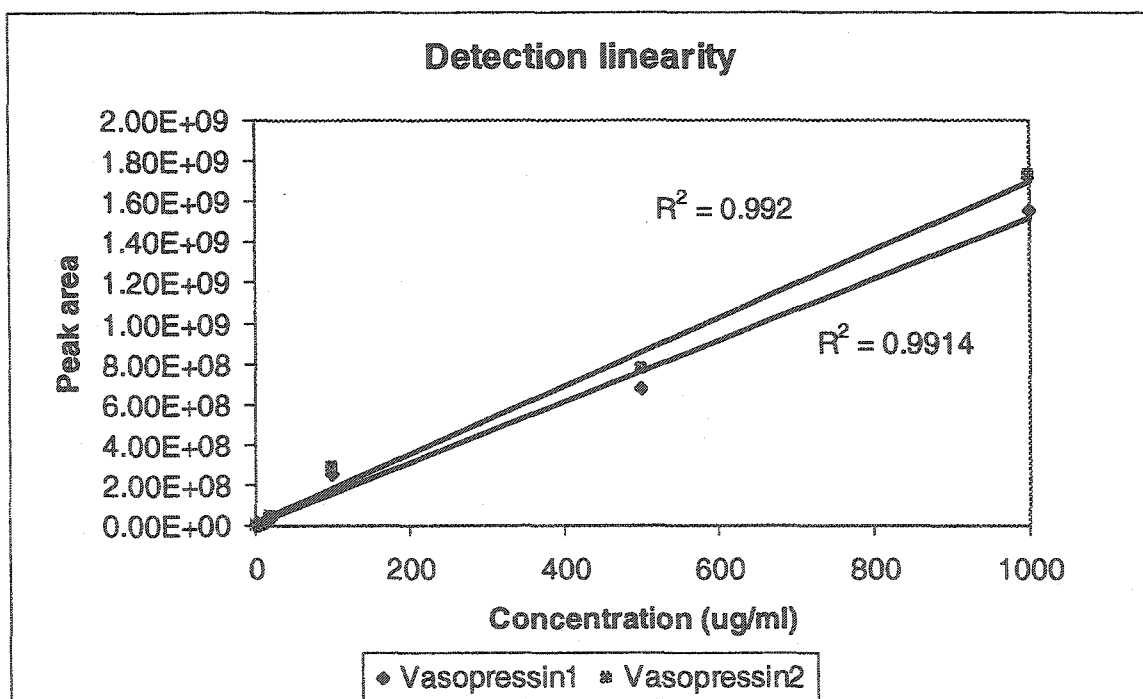


Figure 8. The detection linearity of ESI- MS detection of Vasopressin peptides is shown. Chromatographic conditions are the same as in Figure 6.

## Conclusions

Macrocyclic glycopeptide CSPs have great resolving power for closely related peptides separated by HPLC. In general, (1) terminal polymorphisms produced separations of greater resolution than those occurring in the middle of the peptide (2) substituting a charged amino acid for an uncharged residue produced a separation of greater resolution than exchanging an uncharged amino acid for another uncharged amino acid or substituting like charged amino acids (3) All peptides containing a D-amino acid polymorphism eluted before the corresponding L-amino acid containing peptide. Most of the mobile phase conditions used are MS-compatible and good LOD can be achieved by using ESI/MS. The retention behavior of peptides on macrocyclic glycopeptide CSPs shows U-curve shaped retention versus the concentration of the organic modifier content. Mobile phase composition, including the type and amount of organic modifier, mobile phase pH, and ionic strength, plays an important role in peptide elution and peak shape. The selectivity of the macrocyclic glycopeptide stationary phases for achiral and chiral polymorphisms using ESI-MS compatible mobile phases should broaden their appeal for use in all areas where peptide separations are important.

## Acknowledgements

We gratefully acknowledge the National Institute of Health (NIH R01 GM53825-07) for funding for this research.

## References

- [1] J.U. Bowie, J.F. Reidhaar-Olson, W.A. Lim, R.T. Sauer, *Science* 247 (1990) 1306.



- [2] J.F. Reidhaar-Olson, R.T. Sauer, *Science* 241 (1988) 53.
- [3] J. Suckow, P. Markiewicz, L.G. Kleina, J. Miller, B. Kisters-Woike, B. Müller-Hill, *J. Mol. Biol.* 261 (1996) 509.
- [4] C.L. Gatlin, J.k. Eng, S.T. Cross, J.C. Detter, J.R. Yates III, *Anal. Chem.* 72 (2000) 757.
- [5] D. Chasman, R.M. Adams, *J. Mol. Biol.* 307 (2001) 683.
- [6] P. Liu, F.E. Regnier, *Anal. Chem.* 75 (2003) 4956.
- [7] K. Almind, G. Inoue, O. Pedersen, C.R. Kahn, *J. Clin. Invest.* 97 (1996) 2569.
- [8] M.M. Goodenow, G. Bloom, S.L. Rose, S.M. Pomeroy, P.O. O'Brien, E.E. Perez, J.W. Sleasman, B.M. Dunn<sup>2</sup>, *Virology* 292 (2002) 137.
- [9] L.A. Larsen, P.S. Andersen, J. Kanters, I.H. Svendsen, J.R. Jacobsen, J. Vuust, G. Wettrell, L. Tranebjærg, J. Bathen, M. Christiansen, *Clinical Chemistry* 47 (2001) 1390.
- [10] E. Pietilä, H. Fodstad, E. Niskasaari, P.J. Laitinen, H. Swan, M. Savolainen, Y.A. Kesäniemi, K. Kontula, H.V. Huikuri, *Journal of the American College of Cardiology* 40 (2002) 511.
- [11] C.L. Gatlin, G.R. Kleemann, L.G. Hays, A.J. Link, J.R. Yates, III, *Anal. Biochem.* 263 (1998) 93.
- [12] R. Xiang, C. Horváth, J.A. Wilkins, *Anal. Chem.* 75 (2003) 1819.
- [13] G. Török, A. Péter, E. Vékes, J. Sápi, M. Laronze, J.-Y. Laronze, D.W. Armstrong, *Chromatographic Supplement* 51 (1999) S165.
- [14] A. Péter, G. Török, D.W. Armstrong, G. Tóth, D. Tourwé, *J. Chromtogr. A* 904 (2000) 1.
- [15] A. Péter, E. Olajos, R. Casimir, D. Tourwé, Q.B. Broxterman, B. Kaptein, D.W. Armstrong, *J. Chromtogr. A* 871 (2000) 105.
- [16] A. Péter, L. Lázár, F. Fülöp, D.W. Armstrong, *J. Chromtogr. A* 926 (2001) 229.
- [17] G. Török, A. Péter, D.W. Armstrong, D. Tourwé, G. Tóth, J. Sápi, *Chirality* 13 (2001) 648.
- [18] B.S. Welinder, S. Linde, B. Hansen, *J. Chromtogr.* 361 (1986) 357.
- [19] E. Spindel, D. Pettibone, L. Fisher, J. Feernstrom, R. Wurtman, *J. Chromtogr.* 222 (1981) 381.
- [20] A. Péter, D.W. Armstrong, G. Toth, D. Tourwe, *J. Chromtogr.* 904 (2000) 1.
- [21] A. Péter, G. Toth, W. Van den Nest, G. Laus, D. Tourwe, D.W. Armstrong, *Chromatographia* 48 (1998) 53.
- [22] A. Peter, G. Török, D.W. Armstrong, *J. Chromtogr.* 793 (1998) 283.
- [23] G.J. Opiteck, J. W. Jorgenson, *Anal. Chem.* 69 (1997) 2283.
- [24] M. Dizdaroglu, M.G. Simic, F. Rioux, S. St-Pierre, *J. Chromtogr.* 245 (1982) 158.
- [25] C.T. Mant, R.S. Hodges, *J. Chromtogr.* 397 (1987) 99.
- [26] Cs. Horvath, W. Melander, I. Molnar, P. Molnar, *Anal. Chem.* 49 (1977) 2295.
- [27] C.T. Mant, R.S. Hodges, *J. Chromtogr.* 327 (1985) 147.
- [28] W.S. Hancock, C.A. Bishop, J.E. Battersby, D.R.K. Harding, M.T.W. Hearn, *J. Chromtogr.* 168 (1979) 377.
- [29] D. Guo, C.T. Mant, R.S. Hodges, *J. Chromtogr.* 386 (1987) 205.
- [30] H.K. Ekborg-Ott, Y. Liu, D.W. Armstrong, *Chirality* 10 (1998) 434.
- [31] A. Berthod, Y. Liu, C. Bagwill, D.W. Armstrong, *J. Chromtogr.* 731 (1996) 123.

- [32] H.P.J. Bennett, *J. Chromtogr.* 226 (1983) 501.
- [33] D.W. Armstrong; Y. Liu; H.K. Ekborgott, *Chirality* 7 (1995) 474.
- [34] D.W. Armstrong; Y. Tang; S. Chen, Y. Zhou, C. Bagwill, J. Chen, *Anal. Chem.* 66 (1994) 1690.
- [35] M. Mann, R.C. Hendrickson, P. Akhilesh, *Annu. Rev. Biochem.* 70 (2001) 437.
- [36] B. Larsen, V. Viswanatha, S.Y. Chang, V.J. Hruby, *J. Chromtogr. Sci.* 16 (1978) 207.
- [37] J. Charvátová, V. Kašicka, T. Barth, Z. Deyl, I. Mikšlk, V. Král, *J. Chromtogr. A* 1009 (2003) 73.
- [38] B.L. Currie, J. Chang, R. Cooley, *J. Liq. Chromatogr.* 3 (1980) 513.
- [39] T. Stroink, G. Wiese, J. Teeuwesen, H. Lingeman, J.C.M. Waterval, A. Bult, G.J. de Jong, W.J.M. Underberg, *J. Pharm. Biomed. Anal.* 30 (2002) 1393.
- [40] R. S. Blanquet, K.H. Bui, D.W. Armstrong, *J. Liq. Chromatogr.* 9 (1986) 1933.
- [41] D.W. Armstrong, R.E. Boehm, *J. Chromatogr. Sci.* 22 (1984) 378.
- [42] R.J. Simpson, R.L. Moritz, *J. Chromatogr.* 474 (1989) 418.
- [43] A.W. Purcell, G.L. Zhao, M.I. Aguilar, M.T.W. Hearn, *J. Chromatogr. A* 852 (1999) 43.
- [44] A.W. Purcell, M. Aguilar, M.T. W. Hearn, *Anal. Chem.* 65 (1993) 3038.
- [45] D.W. Lee, B.Y. Cho, *J. Liq. Chromatogr.* 17 (1994) 2541.
- [46] E. Krause, M. Beyermann, M. Dathe, S. Rothmund, M. Bienert, *Anal. Chem.* 67 (1995) 252.
- [47] F. Lin, W. Chen, M.T.W. Hearn, *J. Mol. Recognit.* 15 (2002) 55.
- [48] E.B. Klaas, Cs. Horvath, W.R. Melander, A. Nahum, *J. Chromtogr.* 203 (1981) 65.
- [49] K. Krummen, *J. Liq. Chromtogr.* 3 (1980) 1243.
- [50] J.E. Rivier, *J. Liq. Chromtogr.* 1 (1978) 343.
- [51] N. Takahashi, N. Ishioka, Y. Takahashi, F. W. Putam, *J. Chromtogr.* 326 (1985) 407.
- [52] T. Sasagawa, T. Okuyama, D.C. Teller, *J. Chromtogr.* 240 (1982) 329.
- [53] M.J. Desai, D.W. Armstrong, *J. Mass Spectrom.* 9 (2004) 177.
- [54] K.L. Rundlett, D.W. Armstrong, *Anal. Chem.* 68 (1996) 3493.
- [55] D. Zhang, L. Wu, K.J. Koch, R.G. Cooks, *Eur. Mass Spectrom.* 5 (1999) 353

**PART II. CHROMATOGRAPHIC ANALYSIS AND  
CHARACTERIZATION OF MICROBES**

## CHAPTER 4. INTRODUCTION

The traditional method to identify bacteria and other microorganisms involves serial dilution and growing a pure culture. Culturing different type of microbes can take hours, days or weeks. This process generally is labor intensive and contamination prone. In addition, only a small percentage of all known microorganisms are culturable<sup>1</sup>. New methods, new techniques are in need to address the problem. Species can be identified by their inherent DNA differences. Polymerase chain reaction (PCR) assay was developed to analyze microorganisms by comparing their DNA information without isolating a pure culture. It has been widely used in various research fields because of its small sample consumption and high sensitivity<sup>2</sup>. However the original DNA extraction and purification from target cells is still a tedious process. Cell surface property differences have also been used to characterize microorganisms. For example, gram positive, gram negative or acid-fast bacteria can be differentiated by staining with different dyes or combinations of dyes<sup>1</sup>. However, this method also requires large quantities of sample and only provides a very rough classification. Capillary electrophoresis (CE) has been used to separate microorganisms according to their different cell wall chemistry by Armstrong group since 1999<sup>3-5</sup>. When combined with laser-induced fluorescence detection (LIF), cell viability information also can be obtained by this CE approach<sup>6</sup>. Much attention has been drawn to this technique due to its minimal sample consumption and fast analysis time. Desai and Rodriguez recently reviewed research in this field<sup>7, 8</sup>. Affinity based cell separations exploit biospecific interactions between ligands and receptors. Ligand selectivity and dissociation constant are the most important considerations in this approach. Sharma reviewed the early age affinity chromatography for cell

separations<sup>9</sup>. Magnetic cell separation (MACS) is a successful application of this concept<sup>10</sup>. However, multivalent interactions and difficult recoveries are common problems with immunomagnetic separations<sup>11</sup>. Some researchers have tried using field flow fractionation (FFF) to resolve microbes<sup>12-16</sup>. When an eluent carrying different samples is acted on by a perpendicular field, migration differences can be generated. Sedimentation, thermal, electrical or combinations of fields are common used<sup>12-16</sup>. Unfortunately FFF separations suffer from low resolution due to a combination of poor efficiency and low selectivity<sup>7</sup>.

Using microbes in environmental remediation has become increasingly important. Sakaguchi investigated 83 different microorganisms for heavy metal accumulation<sup>17</sup>. Filtration and centrifugation followed by separate analysis of the cell and liquid fractions are common methods used to evaluate the remediation process<sup>17,18</sup>. Such physical separation procedures are slow and do not provide on-line information. Obviously, a fast, general method to determine heavy metal incorporation by such bacteria would be important.

High performance liquid chromatography (HPLC) was generally used to separate molecules. But it can be used to isolate microbes from culture media or their surroundings. In the second part of dissertation, a novel HPLC column was developed to separate cells from large proteins and other macromolecules (e.g., carbohydrates) present in the nutrient broth, as well as from small molecules. The close packing theory of spheres was introduced to explain the relationship between particle size and the associated void space. When this system is coupled with an ICPMS, real time information on cell uptake of heavy metals can be obtained.

**References**

- (1) Black, J. G. *Microbiology: principles and explorations*, 5th ed.; John Wiley & Sons, 2002.
- (2) P. Belgrader, W. B., D. Hadley, J. Richards, P. Stratton, R. Mariella, F. Milanovich *science* **1999**, *284*, 449-450.
- (3) Daniel W. Armstrong, G. S., J. M. Schneiderheinze, D. J. Westenberg *Anal. Chem.* **1999**, *71*, 5465-5469.
- (4) Daniel W. Armstrong, J. M. S. *Anal. Chem.* **2000**, *72*, 4474-4476.
- (5) Daniel W. Armstrong, J. M. S., J. P. Kullman, L. He *FEMS Microbiol. Lett.* **2001**, *194*, 33-37.
- (6) L. He, R. J. J., L.E. Evans, D.W. Armstrong *Anal. Chem.* **2003**, *75*, 825-834.
- (7) Meera J. Desai, D. W. A. *MMBR* **2003**, *67*, 38-51.
- (8) Michael A. Rodriguez, D. W. A. *J. Chromatogr. A* **2004**, *800*, 7-25.
- (9) Sharma, S. K., Mahendroo, P. P. *J. Chromatogr. A* **1980**, *184*, 471-499.
- (10) Olsvik, O. e. a. *Crit. Microbiol. Rev.* **1994**, *7*, 43-54.
- (11) Hubble, J. *Trends in Biotechnology* **1997**, *15*, 249-255.
- (12) Sharma, R., R. T. Edwards, R. Beckett *Water Res.* **1998**, *32*, 1508-1514.
- (13) Yager, P., M. A. Afromowitz, D. Bell, F. K. Forster, J. P. Holl, A. Kamholz, B. Weigla. *Proc. SPIE-Int. Soc. Opt. Eng.* **1988**, 3515.
- (14) Khoshmanesh, A., R. Sharma, and R. Beckett. *J. Environ. Eng.* **1997**, *127*, 19-25.
- (15) Jussila, M. A., G. Yohannes, M. L. Riekkola. *J. Microcol. Separ.* **1997**, *9*, 601-609.
- (16) Gao, Y. S., S. C. Lorbach, R. Blake *J. Microcol. Separ.* **1997**, *9*, 497-501.
- (17) Nakajima, A. S., Takashi *Appl. Microbiol. Biotechnol.* **1986**, *24*, 59-64.

- (18) Strandberg, G. W. S., S. E., II; Parrott, J. R., Jr. *Appl. Environ. Microbiol.* 1981, 41, 237.

## CHAPTER 5. FACILE MONITORING AND EVALUATION OF BACTERIA IN A FERMENTATION PROCESS USING PERFUSION CHROMATOGRAPHY AND POLARIMETRY DETECTION

Alain Berthod<sup>3</sup>, Bo Zhang, Daniel W. Armstrong\*

A paper published in Journal of Separation Science  
Iowa State University, Department of Chemistry, Ames, Iowa 50011, USA

### Abstract

A 670 nm diode laser polarimeter was used as a detector for living cells in perfusion chromatography. It was found that all microorganisms examined, including vegetal organisms such as algae and fungi as well as several strains of different bacteria gave a levorotatory signal, producing negative peaks in the chromatograms. Most naturally occurring chiral molecules, such as sugars and amino acids are dextrorotatory and give positive polarimetric peaks. A hydrophilic OH-functionalized polystyrene divinylbenzene spherical porous particle packing was used as a sieving and size exclusion material and packed in 27 x 0.95 cm columns. The theory of the close-packing of spheres is summarized to show that common bacteria should be able to perfuse in the interparticle voids of the 50  $\mu\text{m}$  spherical packing. It is shown that bacteria are eluted with the exclusion volume; a selective permeation of polymer with molecular weight ranging from  $10^3$  to  $2 \times 10^6$  is obtained, and total permeation occurs for small molecules. The restricted access columns are

---

<sup>3</sup> On leave from laboratoire des Sciences Analytiques, CNRS, Université de Lyon 1, CPE Lyon, 69622 Villeurbanne, France

\* Corresponding author, e-mail: sec4dwa@iastate.edu



used to follow the changes in cell concentration in bacteria cultures. The growth of three different bacteria was studied using calibrated polarimetric signal.

Key Words: Perfusion chromatography, close-packing, microbes, direct injection, fermentation, size-exclusion, restricted access.

## 1 Introduction

Biological matrices can be difficult to analyze using HPLC columns. Often time-consuming sample pretreatments are needed to remove cell debris and proteinaceous material that would adsorb onto the column packing and weaken performance or even constrain the mobile phase flow to a degree that the column must be replaced. Biological sample pretreatment was greatly improved by the development of solid phase extraction (SPE) that can be coupled on-line with HPLC [1-3]. Using micellar mobile phases, it is possible to inject biological samples directly because the micelles complex the proteins and greatly limit their adsorption on the column packing [4]. The cost is a reduced efficiency due to slower mass transfer of solutes with the surfactant covered stationary phase.

In 1985, Hagestam and Pinkerton introduced a new bimodal packing for HPLC [5]. They termed it "internal reversed phase packing", but this concept was adopted by the scientific community under the appellation of restricted-access material (RAM) [6-8]. RAM is successfully used for fast analysis of metabolites and drugs in biological fluids [9-11]. These phases are able to separate polymers and macromolecules from the small molecules so well that mass spectrometers can be used as the detector [12]. RAMs are always bimodal. Large entities are excluded from entering the small pores. They elute with or close to the dead volume passing through the interstices between the packing particles. Small molecules

can enter the RAM pores, interact with the internal bonded apolar moieties and can be retained by a conventional mechanism [5, 7-8].

Since 1997, we have been interested in the separation of microorganisms, microbes, bacteria or fungi, using tools usually reserved for molecules. In our first article on this topic, we showed that capillary electrophoresis (CE) and capillary isoelectric focusing could be useful tools to effectively separate microorganisms [13]. Extending the CE studies, we showed that microbe identification was possible [14-15]. Unfortunately, traditional columns filled with RAM packing will not be able to separate large proteins and/or macromolecules from bacteria. They will just segregate the smaller molecules. Since we needed to separate the cells from large proteins and other macromolecules (e.g. carbohydrates) present in the nutrient broth and from the small molecules, we thought to use the interstitial spaces between particles to let the cells pass through and a polar perfusion chromatography material to retain macromolecules and small molecules [16].

In this work, the close-packing arrangement of hard spheres is reviewed in order to examine the dimensions of the interstitial voids in the packing of spherical particles. Next, the capability of a column packed with an appropriate size perfusion chromatography material is evaluated to separate microbes from other material present in a culture medium. The technique is then applied to follow the microbial fermentation in several cultures of different conditions.

## 2 Material and methods

### 2.1 Chemicals

Buffer solutions were prepared with tromethamine (TRIS or tri(hydroxymethyl) aminomethane), m.w. 121,  $pK_a = 5.7$ , and boric acid, m.w. 62,  $pK_{a1} = 9.14$ ,  $pK_{a2} = 12.74$ ,  $pK_{a3} = 13.8$ . Disodium ethylenediaminetetraacetate (EDTA), m.w. 336, was used to chelate any heavy metal ions. They were obtained from Fisher Scientific (Fairlawn, New Jersey, USA). Dextran molecular standards of m.w. 25,000 (25K), 270K, 2,370,000 (2.37M) and 8.72M were obtained from Polymer Standards Service GmbH (Mainz, Germany). All other chemicals were obtained from Sigma-Aldrich (St. Louis, Missouri, USA).

### 2.2 Spherical monodisperse porous packing for perfusion chromatography

The size exclusion packing was POROS® Perfusion chromatography media obtained from PerSeptive (Applied Biosystems, Framingham, Maryland, USA). The 50  $\mu\text{m}$  POROS 50 OH was selected. It is a spherical hydrophilic 50  $\mu\text{m}$  polystyrene divinyl benzene (PS-DVD) based material with two classes of pores. Large 0.5  $\mu\text{m}$  throughpores allow mobile phase flow to go through the particles. Smaller 50-70 nm pores can be accessed from inside the throughpores [16-18]. The PS-DVD internal as well as external surface was coated with a cross-linked polyhydroxylated polymer that renders it homogeneously polar and hydrophilic [19]. The specific surface area is 70 +/- 5  $\text{m}^2/\text{g}$  [18]. The material can withstand pressure of 10 Mpa (100  $\text{kg}/\text{cm}^2$  or 1400 p.s.i.), pH as low as 0 (1M HCl) or as high as 14.7 (5M NaOH), but it is sensitive to oxidizers and reducing agents [19].

### 2.3 Biochemicals

*Bifidobacteria infantis* powder and *Lactobacillus acidophilus* tablets were purchased at the pharmaceutical department of the local Wal Mart drug store. *Escherichia coli* K12 was

obtained from Fluka Chemical Corp. (Milwaukee, Wisconsin, USA). The bacterial nutrient broth for *B. infantis* and *L. acidophilus* was prepared with the DIFCO 234000 concentrate obtained from Becton Dickinson (Sparks, Maryland, USA). The *E. coli* nutrient was prepared with the Luria broth base, Miller, product L1900 from Sigma.

#### 2.4 Column preparation

Stainless steel was avoided because the salt-containing mobile phases rapidly corroded the metal columns and fittings contaminating the biological material by metal ions. A ½" clear polycarbonate tube was used to prepare the columns (1.28 cm o.d., 0.95 cm i.d.). Teflon ½" ferules and adjusters with 1/16" fitting were prepared by the Iowa State University machine shop. The POROS 50 µm particles are delivered as slurry in 20% ethanol in 14 g (dry material) bottles. After particle settling, the ethanolic solution was removed. The wet POROS particles were suspended in 0.5 M NaCl that was poured in a 27x0.95 cm polycarbonate column whose bottom was closed by a 5 µm Teflon frit. After settling, a flow of 0.5 M NaCl solution was used to form the bed. More slurry was added until the bed completely fill the column that was closed by a 5 µm Teflon frit and closed by a top adjuster. It is estimated that close to 6 g of dry material are contained in one 27x0.95 cm column. The maximum recommended flow speed is 1000 cm/s [19]. This speed corresponds to 12 mL/min with our 0.95 cm i.d. column. The column inlet pressure was less than 0.1 Mpa (1 kg/cm<sup>2</sup> or 70 p.s.i.) at 5 mL/min of 0.5 M NaCl aqueous solution.

#### 2.5 Culturing bacteria

*Bifidobacteria infantis* and *Lactobacillus acidophilus* were grown in DIFCO nutrient broth. The broth was prepared by weighting 8 g of yellow powder in 1 L of distilled water. The solution was sterilized by autoclaving for 20 min at 125°C. About 0.1 g of dried bacteria

were added in an Erlenmeyer containing 200 mL of sterilized and cooled nutrient broth. The recipient was covered with an aluminum foil and placed in a shaker (G24 environmental incubator shaker, New Brunswick Scientific, Edison, New Jersey, USA), at 37°C. The shaker was stopped at various time intervals for bacteria concentration control. *Escherichia coli* K12 was grown in a similar manner except that the Luria broth (15.5 g/L) was used.

## 2.6 Chromatographic system

A classical chromatographic system was used. It was composed by a Shimadzu LC10AS pump (Tokyo, Japan), a Rheodyne 5020 low pressure Teflon valve (Supelco, Bellefonte, Pennsylvania, USA), the POROS glass column, a Shimadzu SPD-6A UV detector or a Shimadzu RF-10AXL fluorescence detector or a polarimeter detector. A Shimadzu CR601 Chromatopac integrator recorded the chromatograms. The mobile phases were pure water, TRIS-Boric acid-EDTA (TBE) pH 6.8 buffer (0.55 g TRIS + 0.28 g boric acid + 0.0376 g EDTA per liter or 4.55 mM TRIS-borate buffer and 0.112 mM EDTA)

## 2.7 Polarimeter detector

The polarimeter detector was a PDR-chiral laser detector from PDR-Chiral Inc. (Lake Park, Florida, USA). It monitors continuously the optical activity of the mobile phase using a 670 nm diode laser. The optical cell has path length of 25 mm and a volume of 22  $\mu$ L. The signal can be either positive or negative according to the solute optical activity.

## 3 Sieving by close-packed hard spheres

### 3.1 Comparing sizes

Hydrodynamic chromatography on close-packed spherical non-porous particles was shown previously able to separate macromolecules on the basis of their size [20]. Microbes

are much bigger than macromolecules. Table 1 compares the size, mass and volume of glucose, an example of small molecule, two Dextran polymer molecules and a variety of living organisms ranging from viruses to a red blood cell. It shows that a large polymer such as Dextran 8.72M and the poliovirus have comparable size, volume and weight. However, microbes are five orders of magnitude heavier and bulkier than the heaviest polymer and viruses [21]. There are ten orders of magnitude difference compared to glucose. When diameters are considered, the differences between microbes and viruses/Dextran 8.72M or molecules are only two or four orders of magnitude, respectively. The most important parameter when pumping colloidal size particles, such as microbes, through a packed bed of spheres, is the size of the interstitial spaces. The bed plus its interstitial spaces acts as a particle-sieving medium. Thus, it is important to understand the essential bed parameters involved with the close packing of monodisperse spheres.

### 3.2 The close-packing of spheres

Packed in a plane, spheres arrange themselves so that each sphere is surrounded hexagonally by six others as illustrated by Figure 1A. The smallest motif of the plane layer is a rhombus or lozenge whose sides correspond to the sphere diameter,  $D$ . This rhombus can be further divided in two equilateral triangles containing a complete interstice between three spheres as shown by Figure 1B. The equilateral triangle has an area of  $\sqrt{3} R^2 = \sqrt{3} \frac{D^2}{4}$ , with  $R$ , the particle radius. It contains a half circle of area  $\pi R^2/2$ . So the interstice area is  $R^2(\sqrt{3} - \pi/2)$  that is 0.16125  $R^2$  or 9.31% of the triangle area (Figure 1B). Whatever the particle diameter is, the interstice area is 9.31% of the total surface occupied by the spheres. Figure 1A shows with the unitary rhombus that there are two interstices per sphere. Table 2

also lists the number of holes per  $\text{cm}^2$  for the different sphere sizes. Obviously, when the particle diameter decreases, there is an increasing number of smaller interstices so that the total interstice area remains constant. Simple geometrical considerations show that the radius of the circle inscribed in the interstice is  $R(2\sqrt{3}/3 - 1)$  or  $0.1547 R$  (Figure 1B). Its area is  $0.0752 R^2$ . This circle corresponds to the largest particle size that can go through the closely packed layer of spheres of radius  $R$ . Friction forces may impede a particle of exactly  $0.1547 R$  from passing through the interstice so that this size is really a maximum. Table 2 lists the maximum sieving size that can go through the closely packed layer of spheres of diameter  $D$ . It shows that it is a good practice in HPLC to filter all mobile phases through a  $0.45 \mu\text{m}$  membrane. Any particle larger than  $0.77 \mu\text{m}$  would be trapped at the head of a  $5 \mu\text{m}$  packed column and decrease the column permeability.

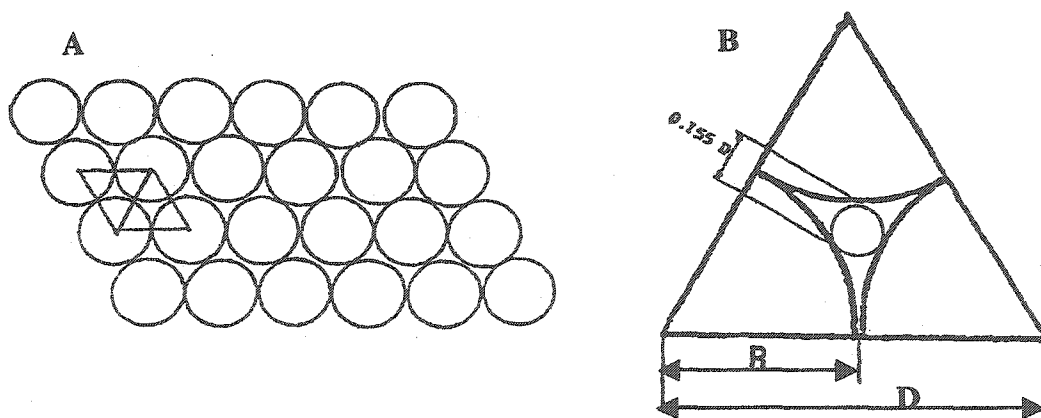


**Figure 1.** Close-packing of non-porous identical hard spheres. A: spheres close packed on a plane. The rhombus delineates the smallest motif. B: The rhombus of A is made of two equilateral triangles containing an interstice whose area is  $0.161R^2$ . The radius of the inscribed circle is  $0.155R$  and its area is  $0.075D^2$ .

Table 1. Comparison of the size, surface area, volume and mass of macromolecules and selected living.

Organism	m.w. <sup>a</sup> (Dalton)	one molecule or cell			1 µg/mL	
		Size <sup>b</sup> (nm)	Volume (µm <sup>3</sup> )	Mass (g)	specific surface (m <sup>2</sup> /g)	nb of entities per mL
glucose	180	0.75	2.2 10 <sup>-10</sup>	3.0 10 <sup>-22</sup>	5800	3.4 10 <sup>+15</sup>
Dextran 25K	25,000	3.8	2.8 10 <sup>-8</sup>	4.2 10 <sup>-20</sup>	1100	2.4 10 <sup>+13</sup>
Dextran 8.72M	8.72 10 <sup>6</sup>	27	1.0 10 <sup>-5</sup>	1.4 10 <sup>-17</sup>	160	6.9 10 <sup>+10</sup>
polio virus	7.83 10 <sup>6</sup>	27	1.0 10 <sup>-5</sup>	1.3 10 <sup>-17</sup>	177	7.7 10 <sup>+10</sup>
tobacco mosaic virus	4.15 10 <sup>7</sup>	15x300	5.3 10 <sup>-5</sup>	6.9 10 <sup>-17</sup>	203	1.5 10 <sup>+10</sup>
bacteriophage T2	2.17 10 <sup>8</sup>	65x90	3.0 10 <sup>-4</sup>	3.6 10 <sup>-16</sup>	53	2.8 10 <sup>+9</sup>
influenza virus	2.53 10 <sup>8</sup>	85	3.2 10 <sup>-4</sup>	4.2 10 <sup>-16</sup>	55	2.4 10 <sup>+9</sup>
pox virus	9.6 10 <sup>9</sup>	230x320	1.3 10 <sup>-2</sup>	1.6 10 <sup>-14</sup>	15	6.4 10 <sup>+7</sup>
Rickettsias	3.7 10 <sup>10</sup>	475	5.6 10 <sup>-2</sup>	6.2 10 <sup>-14</sup>	11.5	1.6 10 <sup>+7</sup>
E. coli	3.5 10 <sup>12</sup>	1300x4000	5.3	5.8 10 <sup>-12</sup>	2.7	1.7 10 <sup>+5</sup>
S. cerevisiae yeast <sup>c</sup>	5.4 10 <sup>13</sup>	5600	90	9 10 <sup>-11</sup>	4.4	11,000
red blood cell	1.2 10 <sup>14</sup>	7000	180	2.0 10 <sup>-10</sup>	0.76	5100

a) for living organisms, theoretical molecular weight obtained multiplying the average organism mass by the Avogadro number.

b) diameter of the (assumed) spherical molecule or particle, or diameter × length for oblong or cylindrical organisms, calculated values using data from [21].

c) highly variable data: a yeast cell can double in size before budding [21].

Figure 2A shows that the second layer of hard spheres occupies the indentations between three spheres of the first layer covering an interstice. However, only one indentation out of two is occupied by a sphere of the second layer. The free indentations of the first layer match an indentation of the second layer (in black on Figure 2A). A particle smaller than 0.1547 D could go through the two layers with a straight path, but through only half the interstices. It could also go through the other interstices following a crooked path.



Table 2. Data on the close packing structure of hard uniform spheres in a cylindrical 10 cm x 4.6 mm tube.

sphere diameter $\mu\text{m}$	maximum sieving size <sup>a</sup> $\mu\text{m}$	number <sup>a</sup> of apertures per $\text{cm}^2$	surface area <sup>b</sup> $\text{m}^2$	driving pressure <sup>c</sup> (1 mL/min)	
				MPa	psi
0.5	0.077	$9.2 \cdot 10^8$	20	630	90,000
1	0.155	$2.3 \cdot 10^8$	10	157	22,500
1.5	0.23	$1.0 \cdot 10^8$	6.6	70	10,000
2	0.31	$5.8 \cdot 10^7$	5	40	5600
5	0.77	$9.2 \cdot 10^6$	2	6.3	900
10	1.55	$2.3 \cdot 10^6$	1	1.8	225
20	3.10	580,000	0.5	0.4	56
50	7.7	92,000	0.2	0.06	9
100	15.5	23,000	0.1	0.015	2.3
200	31	5800	0.05	0.004	0.6
500	77	920	0.02	0.0016	0.1
1000	155	231	0.01	-	-
2000	310	58	0.005	-	-
5000	770 <sup>d</sup>	9 <sup>d</sup>	0.002 <sup>d</sup>	-	-

a) values independent of the column length and diameter

b) values independent of the non porous material density

c) mobile phase viscosity = 0.67 cP (e.g. acetonitrile/water 50/50 % v/v @ 25°C) For any particle diameter, the column dead volume is 0.43 mL that is 26% of the 1.66 mL internal volume of a 10 cm x 4.6 mm cylindrical tube.

d) theoretical value, the 5 mm glass beds would not get into a 4.6 mm cylindrical tube!

Filling a third layer can be done in two ways [22]. The first way is to fill each sphere of the third layer so that it lies directly over a sphere of the first layer, as illustrated by Figure 2B. This way forms the *hexagonal* closest packed structure with the *a-b-a-b* succession of layers. The direct paths through the layer, noted in black on Figure 2, are maintained. The unitary cell is a hexagon with the lozenge base shown in Figure 1A and a height equivalent to the thickness of two layers ( $2\sqrt{2}/3 D$ ). The unitary cell contains two complete spheres. Its volume is  $\sqrt{2} D^3$ . The volume of two spheres is  $2\pi D^3/6$  or  $\pi D^3/3$ . The void space in the

unitary cell is  $(\sqrt{2-\pi/3})D^3 = 0.367D^3$ , that is 25.95% of the whole cell volume. When closely packed in the hexagonal scheme, the spheres occupy 74.05% of the volume, which is the maximum possible with hard uniform spheres.

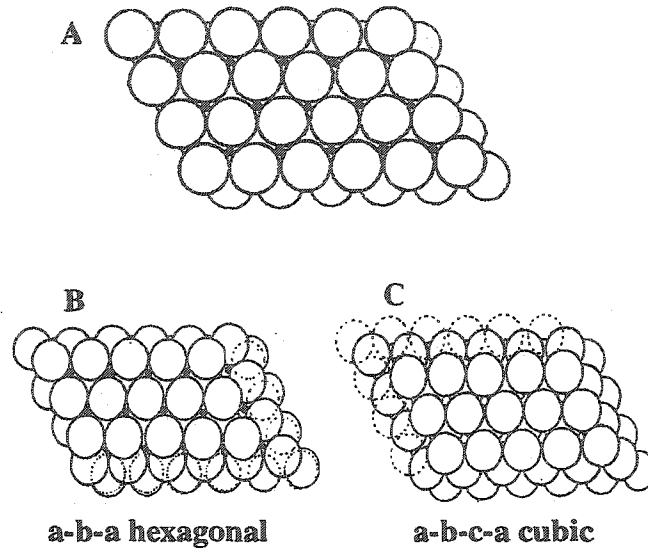


Figure 2. The close-packing of spheres. A: The second sphere layer covers half of the interstice only. There are two ways to add a third layer: B: The hexagonal packing. The third layer covers the first one leaving possible direct paths (in black). C: The cubic packing. The third layer covers the dark spots of A. The dotted spheres belong to the third layers.

The second way to fill the third layer of spheres is to use the dimples that corresponded to the open ways between the two first layers. The succession of layers can be described as *a-b-c-a-b-c*. Figure 2C shows that there is no more direct paths crossing through the three layers. It can be shown that the cell unit is of the face centered cubic type [22]. This way of closely packing spheres is then called the *cubic* closest packed structure. The cell unit contains four spheres. Its side length is  $\sqrt{2} D$ . Its volume is  $2\sqrt{2} D^3$ . The void space in the cell unit is  $2\sqrt{2} D^3 - 4\pi D^3/6 = 0.734 D^3$ , that is again 25.95% of the whole unit cell

volume. Packed in either the hexagonal or the cubic closest packed structure, spheres occupy 74.05% of the volume.

### 3.3 Properties of columns closely packed with non-porous uniform spheres

*Interparticle volume.* When a column is filled by uniform spheres without any interaction between them other than gravity, there is no reason that a layer pattern such as the hexagonal *a-b-a-b* or the cubic *a-b-c-a-b-c* ones forms. Instead, the sphere layers pile up in a random way such as *a-b-c-a-b-a-c-a-b...* This random way can be considered as a succession of cubic and hexagonal layers of thickness equal to three layers or more. Since both arrangements occupy 74% of the total volume, this value is also valid for the random (amorphous) close packing of uniform spheres in a chromatographic column. This means that whatever the particle size is, the interparticle volume of the column is always equal to 26% of the container tube volume, e.g. 0.43 mL for the 10x0.46 cm column of Table 2 or 5.0 mL for the 27x0.95 cm column used in this work.

*Column permeability.* Column permeability is dramatically dependent on the packing particle diameter. The Heigen-Poiseuille equation relates the flow rate,  $F$ , to the driving pressure,  $\Delta P$ , by [23]:

$$F = \frac{\pi r_c^4}{8 L \eta} \Delta P$$

in which  $r_c$  is the radius of an open capillary of length  $L$  and  $\eta$  is the fluid viscosity. As shown by Table 2, the number of possible aperture increase with the square of the sphere diameter, then the pressure needed to get the same flow rate in a packed column is given by [23]:

$$\Delta P = \frac{\Phi \eta FL}{D^2}$$

in which  $\Phi$  is a constant proportional to a dimensionless flow resistance parameter and inversely proportional to the square of the tube diameter.  $D$  is the diameter of the uniform non-porous spheres of the utilized packing material. Table 2 lists the driving pressure needed to obtain a 1 mL/min flow rate in a 10 cm x 4.6 mm column when an acetonitrile-water (50/50% v/v, viscosity 0.67 cP) mobile phase is used at 25°C. With these conditions, the driving pressure becomes too high for classical HPLC pumps when the spheres are smaller than 2  $\mu\text{m}$ . Short columns (3 cm) are used with the 1.5  $\mu\text{m}$  non-porous phases commercially available. 0.08 bar (12 p.s.i.) is the calculated driving pressure with an aqueous mobile phase (1 cP viscosity) at 1 mL/min in the 27x0.95 cm column with 50  $\mu\text{m}$  non-porous spheres.

*Surface Area.* In all porous chromatographic packings, more than 99% of the surface area is due to the internal surface of the pores. With non-porous spheres, the surface area is simply the sphere surface time the number of spheres. The sphere surface is proportional to the square of the sphere diameter, and the number of spheres in a given volume is inversely proportional to the cube of the sphere diameter. So, the surface area in a given volume filled with non-porous spheres depends on the inverse of the sphere diameter. Table 2 lists the surface area of the non-porous spheres contained in the model 10 cm x 4.6 mm column. The surface area of the 27x0.95 cm column filled with 50  $\mu\text{m}$  particles is 1.7  $\text{m}^2$ . The experimental column contains approximately 6 g of POROS. Taking the manufacturer given specific surface (70  $\text{m}^2/\text{g}$ ), the actual surface area of our experimental column is about 400  $\text{m}^2$  showing that 99.5% of this area is internal surface (macro and micro pores) and only 0.5% is external particle surface area

*Interparticle size exclusion capabilities.* The study of the two close packed structures, cubic as well as hexagonal, shows that they contain two types of interstitial sites [22]: octahedral sites and tetrahedral sites. The octahedral sites are surrounded by six spheres whose centers lie at the apices of a regular octahedron. These sites could contain a small sphere of diameter equal or smaller to  $0.414 D$ . There is one octahedral site per sphere in the two possible closely packed structures. The tetrahedral sites are located under and above each sphere that rests on three spheres of the layer below and supports three spheres of the layer above it. There are two tetrahedral sites per sphere. These sites could host a very small sphere of diameter equal or lower than  $0.225 D$ . From a chromatographic point of view, since the size of the interstitial sites are bigger than the apertures between the spheres ( $0.155 D$ ), these apertures give the size of the material than can go through a column closely packed with non-porous beds. However, these columns could be used to separate deformable material such as polymers or cells and a size-exclusion effect will be observed.

#### **4 Evaluation of the perfusion column**

Table 1 shows that most microorganisms fall in the  $0.5-4 \mu\text{m}$  size range. Table 2 shows that  $50 \mu\text{m}$  close-packed particles have a maximum sieving exclusion size of  $7.1 \mu\text{m}$ . Thus, the microbes used in this study should be small enough to penetrate the interstitial spaces between the packing beds. They should be large enough, however, to be unable to access the  $0.4 \mu\text{m}$  throughpores of an individual packing particle. That is why the POROS 50 OH material was selected to prepare the column.

#### 4.1 Molecules and polymers

Molecules and polymers penetrate the large 0.4  $\mu\text{m}$  throughpores (Table 1). Their retention volumes,  $V_r$ , depend on the distribution coefficient,  $K$ , between  $V_p$ , the pore volume or the retention volume of a small molecule penetrating all pores and  $V_i$ , the interparticle volume (mobile) [24]:

$$V_r = V_i + KV_p$$

with  $0 < K < 1$ . Figure 3 shows classical size exclusion chromatography calibration curves for two different 27x0.95 POROS 50 OH column. The exclusion volume is between 7.5 and 8 mL that is 1.5 to 2 mL (20-25%) bigger than the 5-mL theoretical interparticle 7.5 and 8 mL that is 1.5 to 2 mL (20-25%) bigger than the 5-mL theoretical interparticle volume for close-packed spheres. This is due to the polydispersity of POROS sphere that precludes a perfect close-packing structure. The total permeation volume is 16 mL, with a 0.3 mL variation between columns. It means that the volume of the pores is about 8.2 mL or 60% of the packing volume [18,19]. The throughpores make about 45% of the pore volume [18].

Figure 3 shows that molecules heavier than 2 million Daltons are completely excluded for the pore volume. The  $2 \times 10^6$  mass for a dextran polymer corresponds to a 17 nm particle size. Since all known bacteria are bigger than 17 nm (Table 1), it means that they will elute at the exclusion volume. Clearly, it will not be possible to distinguish between two different types of bacteria on the basis of size with this stationary phase. However, bacteria can be separated from both large molecule contaminants (e.g. proteins) and small molecules. It would also be possible to separate very large microorganisms and/or particles (diameters > 7-8  $\mu\text{m}$ ) from the typical size ones (0.5-4  $\mu\text{m}$  diameter) used in this study, since the larger particles would collect at the head of the column.

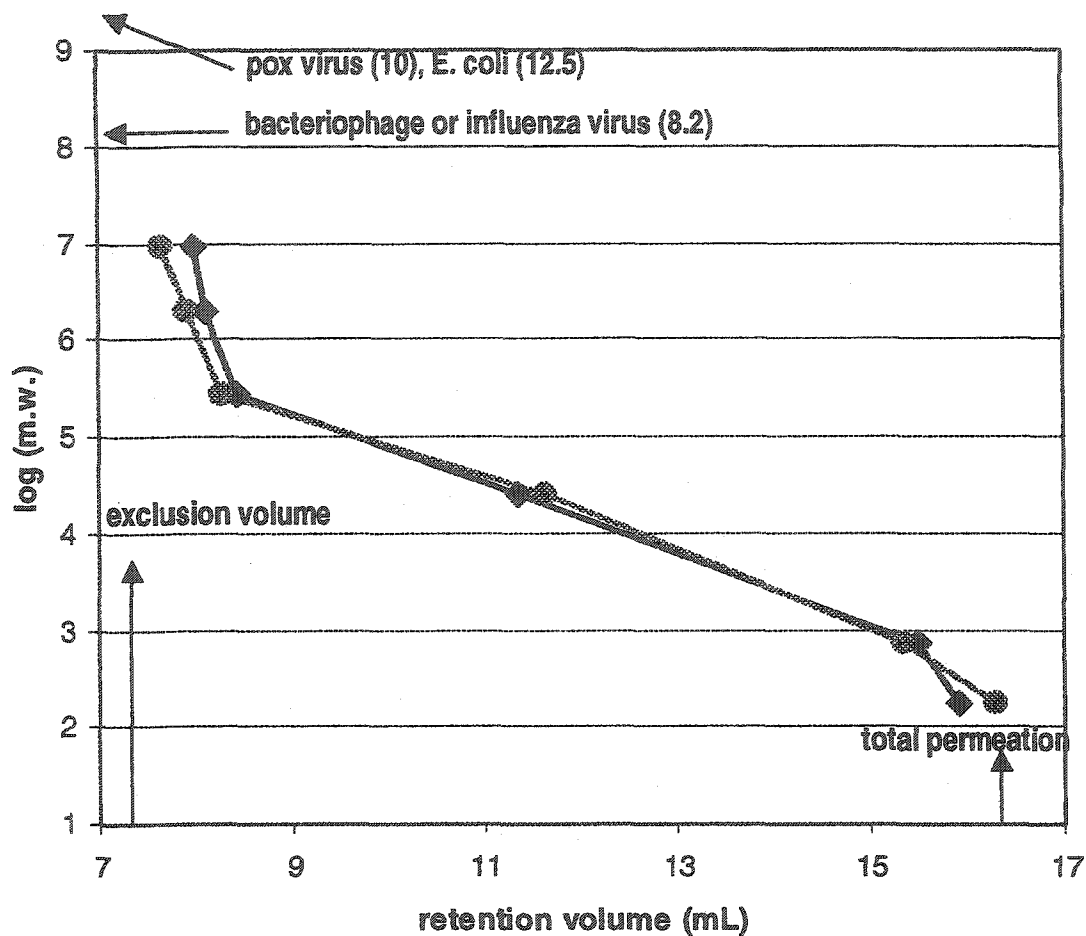


Figure 3. Size exclusion calibration curves of two 27 x 0.95 cm polycarbonate column filled with POROS 50 OH restricted access material. All microorganisms are eluted with the exclusion volume. Theoretical molecular weights of organisms listed in Table 1.

#### 4.2 Bacteria

*Polarimetric detection.* The polarimeter detector continuously measures the optical activity of the mobile phase. It is very selective since it does not detect optically inactive solutes. The extremely interesting result that was found is that microorganisms gave a negative polarimetric signal. Vegetal microorganisms such as algae, or fungi such as yeast (12 strains tested) as well as bacteria such as *Bifidum infantis*, *Micrococcus luteus*, *Escherichia coli* (K12, 9637, 11303, 233499 and 23501 strains tested), *Enterobacter*

*aerogenes*, *Pseudomonas fluorescens*, *Lactobacillus acidophilus* and *Staphylococcus saprophyticus*, all gave negative peaks when detected by polarimetry. Glucose, maltodextrin and the dextran polymers gave positive polarimetric peaks. It was checked that L-glucose, the non-natural enantiomer of natural D-glucose, did produce a negative peak. Since natural sugars, natural amino acids and their combinations are dextrorotatory (positive polarimetric peak), it is unclear why microorganisms are levorotatory (negative polarimetric peak). This property can be used to selectively identify microorganisms. In the case of complex mixtures such as a fermentation broth, the polarimeter detector gives useful information in detecting microorganisms as negative peaks.

*Calibration curves.* An Artek electronic cell counter was used to measure the number of cells per mL contained in different samples. Known amounts of bacteria were injected into the chromatographic system to study the polarimeter detector response versus the number of cells injected under different conditions. *Saccharomyces cerevisiae* (baker's yeast) never eluted through the column. Its size (~6  $\mu\text{m}$  diameter) is too big to percolate from the interstices of the POROS spheres (Table 1).

With A, the polarimetric peak area (at 1 mL/min TBE buffer and 670 nm diode laser), and C, the cell number (cell per mL) in the injected solution (100  $\mu\text{L}$  injection volume), the calibration curve for *Bifidum infantis* was:

$$A = 6.2 \times 10^{-7} C - 12.6$$

$$n = 6, r^2 = 0.996$$

with  $C < 3.9 \times 10^8$  cell/mL. For *Lactobacillus acidophilus*, it was:

$$A = 1.2 \times 10^{-6} C - 18.2$$

$$n = 7, r^2 = 0.993$$



with  $C < 5.5 \times 10^8$  cell/mL, and for *Escherichia coli*, it was:

$$A = 1.7 \times 10^{-6} C - 23.8$$

$$n = 6, r^2 = 0.997$$

with  $C < 4.5 \times 10^8$  cell/mL. The maximum concentrations indicated correspond to cell concentrations obtained at the climax of the bacteria growth curves. It is possible that the polarimetric detector gives a linear response for higher cell concentrations but this could not be tested.

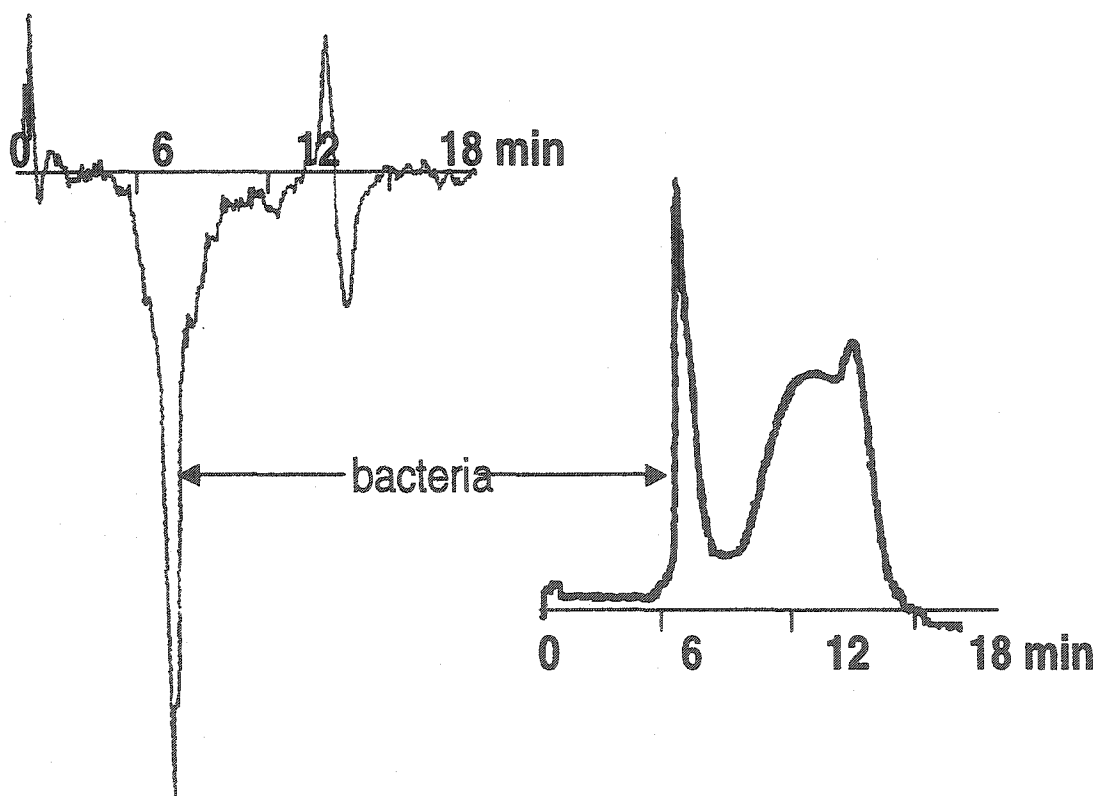


Figure 4. Perfusion chromatogram of a 16-hour old fermentation broth of *Lactobacillus acidophilus*. Cell concentration  $\sim 2.7 \times 10^8$  cell/mL, injection volume 100  $\mu$ L, column 27x0.95 cm POROS 50 OH, mobile phase TBE buffer 1 mL/min, left: polarimetric detection 670 nm diode laser, right: UV 254 nm detection. Note the difference in noise baseline.

The negative intercepts mean that the polarimetric detector needs a minimum cell concentration to give a signal. These minimum concentrations are  $2 \times 10^7$  cell/mL,  $1.5 \times 10^7$  cell/mL and  $1.4 \times 10^7$  cell/mL for *B. infantis*, *L. acidophilus* and *E. coli*, respectively. Figure 4 shows the chromatograms obtained with the same sample of *L. acidophilus* and the polarimetric detector or a UV detector. With the polarimeter detector, the negative peak around 7 min corresponds to the excluded bacteria, it is easily distinguished from the positive and negative peaks showing close to the total permeation volume and corresponding probably to sugars and amino acids in the fermentation broth. With the UV detector, the bacteria peak is also clearly visible, but a broad peak of UV absorbing macromolecules and molecules, corresponding to the nutrients in the fermentation broth, may bias the bacteria peak integration. UV detection is more sensitive than polarimetry. It can be used if the sample is cleaned before injection. The bacteria must be separated from the nutrient medium by at least two cycles: centrifugation, cell pelleting, cleaning and cell resuspension. Obviously, the cleaning procedure will increase the analysis duration. Refractive index and fluorescence (with appropriately stained cells) detections also could be used. Polarimetry was used to follow the bacteria' growth curves.

*Growth curves.* Bacteria growth curves are characterized by four phases. 1) First, there is the LAG phase during which the growth is very slow, while the bacteria acclimate to the food and nutrients in their new habitat. 2) Once the metabolic machinery is running, the LOG phase starts with an exponential increase in cell number. 3) As more and more cells are competing for dwindling food and nutrients, rapid growth stops, a relative stationary state exists when the number of bacteria stabilizes. 4) The final death phase terminates the process when toxic waste products build up and food is depleted. The number of cells decreases.

Figure 5 shows selected chromatograms obtained with polarimetric detection and used to prepare the growth curve of the bacteria *Bifidum infantis*. At the indicated times, 1 mL of the culture is collected from the 200 mL Erlenmeyer with a sterile medical syringe. It is diluted with 4 mL of mobile phase (TBE buffer or 8.5 g/L NaCl aqueous solution). 100  $\mu$ L are directly injected on the 27 x 0.95 cm POROS column to obtain in 15 min the chromatograms shown by Fig. 5.

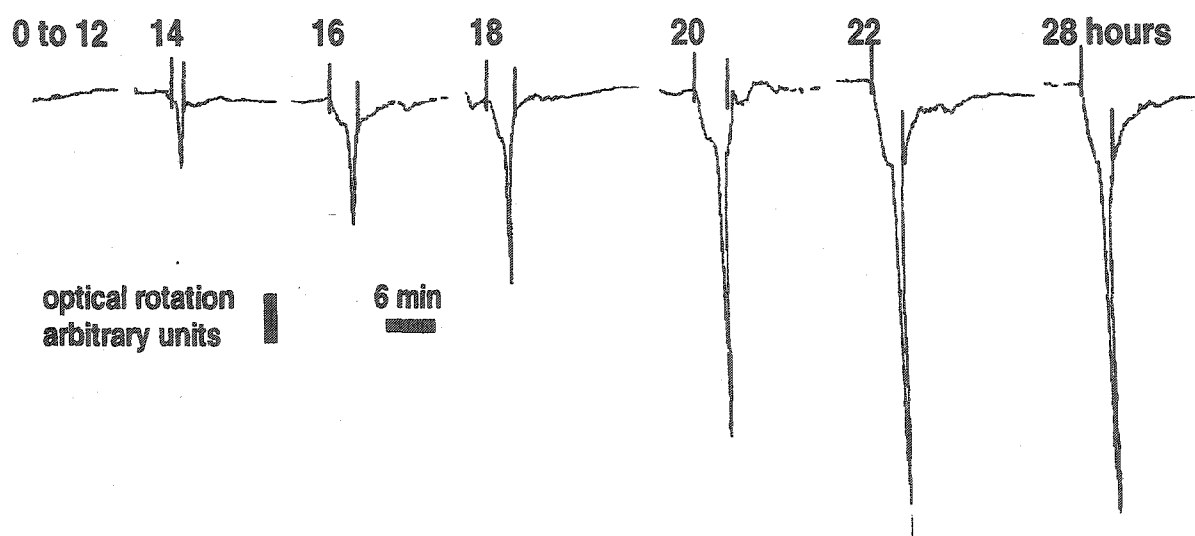


Figure 5. Chromatograms of a culture of *Bifidum infantis* obtained after different culture times. Culture medium: DIFCO nutrient broth, culture temperature: 37°C, in New Brunswick G24 incubator shaker. Column POROS 50 OH, 27 x 0.95 cm, mobile phase 100% TBE buffer 1 mL/min, injection of 100  $\mu$ L (20  $\mu$ L broth + 80  $\mu$ L buffer), polarimetric detector. The vertical markers delineate the integration start and end.

Figure 6 shows the growth curves for three different bacteria. The four life phases are clearly observed. From a chemical point of view, the reproducibility of cell culture is low. When exactly the same volume of nutrient medium is prepared, seeded with the same mass of dry bacteria (ratio live/dead unknown and time depending), and cultured in the incubator at the same rotation speed and temperature, LAG times and/or maximum cell

concentrations differing by more than 40% may be obtained. Taking in account the result variability, it can just be said that, at 37°C, the LAG time of *E. coli* is shorter than that of *L. acidophilus* and *B. infantis*.

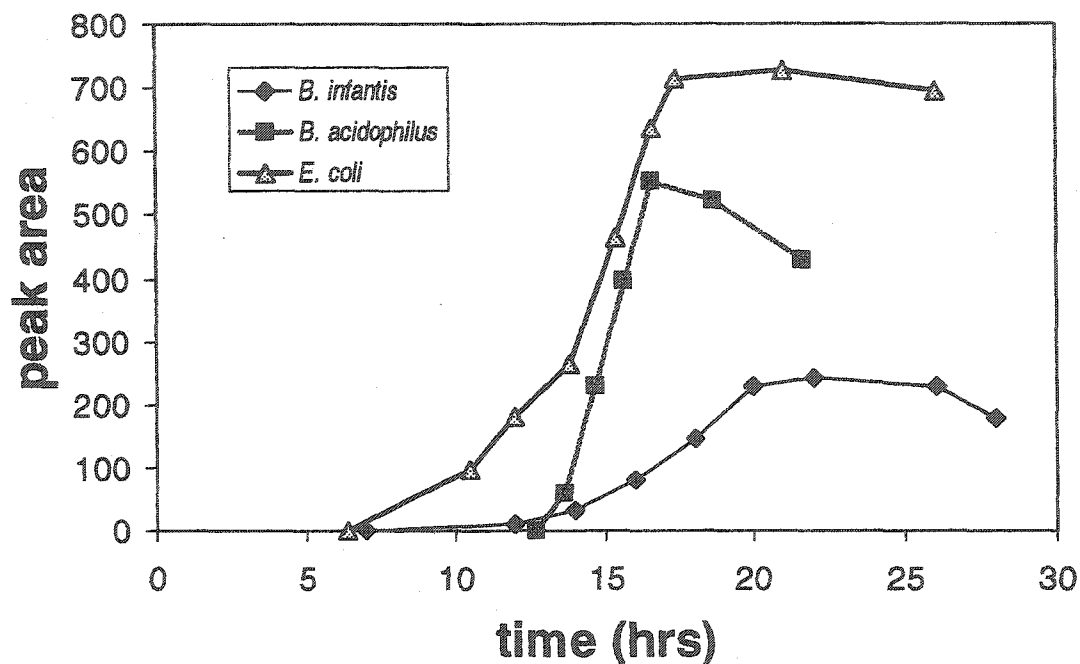


Figure 6. Growth curves of three different bacteria followed by perfusion chromatography and polarimetric detection. Diamonds: *Bifidum infantis* grown in DIFCO nutrient broth; squares: *Lactobacillus acidophilus* (in DIFCO nutrient broth) and triangles: *Escherichia coli* (in Luria broth).

## Conclusions

Two points should be stressed concerning this work: 1) microorganisms give a negative response with polarimetric detection while most natural optically active small molecules and macromolecules give a positive response. This can be used to selectively detect and quantitate microorganisms. 2) The perfusion polystyrene divinyl benzene packing material with spherical polar particles, large throughpores and small pores, can be used to quickly separate the large microorganisms by total exclusion from the macromolecules and

from the small molecules that penetrate the porous spheres. The association of perfusion chromatography with polarimetric detection can accelerate the off-line monitoring and control of industrial fermentation broths. Small modifications would allow on-line measurements.

### Acknowledgments

Support by the National Institute of Health NIH R01 GM 53825 is gratefully acknowledged. AB thanks the French Centre National de la Recherche Scientifique (UMR5619 ERS2007 FRE2496) for a one-year sabbatical leave at ISU.

### References

- [1] D.T. Rossi, N. Zhang, *J. Chromatogr. A* **2000**, *885*, 97-113.
- [2] M.C. Hennion, *J. Chromatogr. A* **1999**, *856*, 3-54.
- [3] L.A. Berrueta, B. Gallo, F. Vincente, *Chromatographia* **1995**, *40*, 474-483.
- [4] A. Berthod, C. Garcia Alvarez-Coque, *Micellar Liquid Chromatography*, Chromatogr. Sci. Ser. 83, Marcel Dekker, New York 2000.
- [5] H. Hegestam, T.C. Pinkerton, *Anal. Chem.* **1985**, *57*, 1757-1763.
- [6] D. Westerlung, *Chromatographia* **1987**, *24*, 155-164.
- [7] J. Haginaka, *Trends Anal. Chem.* **1991**, *10*, 17-22.
- [8] K.K. Unger, *Chromatographia* **1991**, *31*, 507-511.
- [9] W.M. Mullett, J. Pawliszyn, *Anal. Chem.* **2002**, *74*, 1081-1087.
- [10] P. Chiap, A. Ceccato, R. Gora, P. Hubert, J. Geczy, J. Crommen, *J. Pharm. Biomed. Anal.* **2001**, *27*, 447-455.
- [11] E. Blahova, L. Bovanova, E. Brandsteterova, *J. Liq. Chromatogr. & Rel. Technol.* **2001**, *24*, 3027-3035.
- [12] D. Ortelli, S. Rudaz, S. Souverain, J.L. Veuthey, *J. Sep. Sci.* **2002**, *25*, 222-228.
- [13] D.W. Armstrong, G. Schulte, J.M. Schneiderheinze, D.J. Westenberg, *Anal. Chem.* **1999**, *71*, 5465-5469.
- [14] D.W. Armstrong, J.M. Schneiderheinze, *Anal. Chem.* **2000**, *72*, 4474-4476.
- [15] D.W. Armstrong, J.M. Schneiderheinze, J.P. Kullman, L. He, *FEMS Microbiol. Lett.* **2001**, *194*, 33-37.

- [16] N.B. Afeyan, N.F. Gordon, I. Mazsaroff, L. Varady, S.P. Fulton, Y.B. Yang, F.E. Regnier, *J. Chromatogr.*, **1990**, *519*, 1-29.
- [17] M. McCoy, K. Kalghatgi, F.E. Regnier, N.B. Afeyan, *J. Chromatogr.*, **1996**, *743*, 221-229.
- [18] D. Whitney, M. McCoy, N. Gordon, N.B. Afeyan, *J. Chromatogr.*, **1998**, *807*, 165-184.
- [19] POROS® 50 OH Operating instructions, PerSeptive Biosystems part number 8-0106-40-0295, rev. 4, 1997.
- [20] G. Stegeman, R. Oostervink, J.C. Kraak, H. Poppe, *J. Chromatogr.*, **1990**, *506*, 547-561.
- [21] L.M. Prescott, J.P. Harley, D.A. Klein, *Microbiology*, 3<sup>rd</sup> Ed., W.C. Brown Publishers, Dubuque, Iowa, 1996.
- [22] R.A. Alberty, R.J. Silbey, *Physical Chemistry*, Wiley, New York, 1992.
- [23] J.C. Giddings, *Unified Separation Science*, Wiley, New York, 1991.
- [24] C.Y. Kuo, T. Provder, in *Data Analysis in Size Exclusion Chromatography*, T. Provder (Ed.), ACS Symposium Ser., **1987**, *352*, 2-28.

## **CHAPTER 6. PORE Exclusion Chromatography-Inductively Coupled Plasma-Mass Spectrometry for Monitoring Elements in Bacteria: A Study on Microbial Removal of Uranium from Aqueous Solution**

Bo Zhang, Fumin Li, R. S. Houk, and Daniel W. Armstrong\*

A paper published in *Analytical Chemistry*

*Department of Chemistry, Ames Laboratory-U.S. Department of Energy, Iowa State University, Ames, Iowa 50011*

### **Abstract**

The interstitial spaces between spherical particles in a packed column can act as a sieve that passes microorganisms below a certain size. If the bed is a perfusion-type material (containing a binary distribution of large and small pores), colloidal-size microorganisms are subject only to pore exclusion, while all molecules are subject to size exclusion among the various pores. Thus, microorganisms elute first, followed by macromolecules, and then small molecules. Coupling this separation method to an ICP magnetic sector mass spectrometer provides a sensitive, direct means to study the microbial uptake of heavy metals (i.e., uranium) from their surrounding environments. Multiple metal ions can be monitored in the microorganism and in the surrounding solution. In this way, definitive information can be provided for the remediation of radioactive waste sites. The effect of uranium on microbial growth is also discussed.

---

\* Corresponding author. Phone: 515-294-1394. Fax: 515-294-0838. E-mail: sec4dwa@iastate.edu.

Uranium is the origin of all fissionable material and is thus a key element in the nuclear energy industry. Reserves of uranium oxide are estimated to be  $\sim 6 \times 10^8$  kg.<sup>1</sup> Complete processing of these deposits would produce  $\sim 10^{12}$  kg of solid waste and  $\sim 10^9$  m<sup>3</sup> of liquid waste.<sup>2-5</sup> Liquid waste poses the greatest treatment problem, as much from its large volume as its radioactivity. These solutions also contain other toxic metals and hazardous chemicals<sup>2-9</sup>. They are typically stored in large impoundments. In 1979, in Church Rock, NM, the dam of such an impoundment broke and sent  $\sim 10^5$  m<sup>3</sup> of wastewater into a local area.<sup>2</sup> Thus, remediating uranium from liquid waste impoundments is a key environmental problem.

Various approaches for removing uranium from such reservoirs have been reported. Chemical or physical removal can be done by ion exchange<sup>10</sup>, zeolites,<sup>11</sup> silica gel,<sup>12</sup> and derivatized polymers.<sup>13,14</sup> Deliberate uptake of uranium by biomass or microbes is another important approach. Microbes studied specifically for uranium removal include spent brewery yeast,<sup>15</sup> *Desulfovibrio desulfuricans*,<sup>16</sup> *Pseudomonas aeruginosa*,<sup>17</sup> *Bacillus subtilis*,<sup>18</sup> and *Shewanella putrefaciens*.<sup>19</sup> Sakaguchi<sup>20</sup> investigated 83 different microorganisms for heavy metal accumulation.

Obviously, a fast, general method to determine heavy metal incorporation by such bacteria is desirable. Filtration and centrifugation followed by separate analysis of the cell and liquid fractions are common methods.<sup>20,21</sup> Such physical separation procedures are slow and do not provide on-line information. Recently, Armstrong and co-workers developed a variation of size exclusion chromatography that can separate cells from large molecules (e.g., proteins) and small molecules.<sup>22</sup> Large cells elute first and can be resolved from both large and small molecular components in a few minutes.



In the present work, we couple this pore exclusion/size exclusion chromatography separation with element-selective detection by an inductively coupled plasma magnetic sector mass spectrometer (ICPMS). Various workers have shown ICPMS is a valuable detection method for inorganic elements in proteins,<sup>23</sup> DNA,<sup>24</sup> and other molecules separated by size exclusion chromatography. These previous detection methods were not designed to examine the elemental content of intact microbes. Desirable features of ICPMS as a chromatographic detection method include very good detection limits, multielement capability, and the ability to measure particular isotopes. This combined method is tested here for monitoring uranium in *B. subtilis*<sup>19,25</sup> and *S. putrefaciens*,<sup>17,20,26</sup> which can readily bind uranium from solution. These bacteria are easy to obtain and culture and are not pathogenic to humans.

## **1 Experimental section**

### **1.1 Chemicals and Materials**

Disodium ethylenediaminetetraacetate (EDTA) was obtained from Fisher Scientific (Fairlawn, NJ). Deionized water (18 M $\Omega$  cm<sup>-1</sup>, 25 °C) was produced by a Nanopure II system (Barnstead, Newton, MA). The bacterial nutrient broth was prepared from DIFCO 234000 concentrate (Becton Dickinson, Sparks, MD). All other chemicals were from Sigma Aldrich (St. Louis, MO). Uranium stock solution was prepared from a 1000 ppm ICP standard in 2% aqueous HNO<sub>3</sub> (Plasmachem Associates, Bradley Beach, NJ). Trisodium citrate was added at 500 g L<sup>-1</sup>, and the pH was adjusted to 7.0 with 1 M NaOH. The concentration of uranium in the stock solution was 640 ppm.

The aqueous chemistry of uranium is complex. Uranyl ion ( $\text{UO}_2^{2+}$ ) is expected to be the main soluble form of uranium in solutions at neutral or high pH. In citrate solution, uranyl ion can form a variety of polynuclear complexes.<sup>27,28</sup> The exact chemical form of the uranium in the growth medium was not determined.

Safety note: the solutions in this study contain uranium, especially the stock solution and the spiked growth medium. They should be handled with gloves in containers labeled for radioactive materials. Waste solution should also be labeled to contain uranium.

## 1.2 Bacteria Growth and Counting

DIFCO nutrient broth powder was dissolved at  $8 \text{ g L}^{-1}$  in deionized water. All culture media were autoclaved at  $121^\circ \text{C}$ . *B. subtilis* or *S. putrefaciens* were inoculated into 200 mL of growth medium in an autoclaved 250-mL Erlenmeyer flask. The flask was covered with aluminum foil and placed in a shaker (model G24, New Brunswick Scientific, Edison, NJ) at  $37^\circ \text{C}$ . The shaker was stopped at various time intervals for sampling. Cell pellets were resuspended into 0.17% aqueous NaCl. Cells were washed three times with this solution before injection onto the column. In some experiments, uranium was added at 14 ppm to the nutrient broth. Cells were harvested during the log growth phase, except where stated otherwise.

Cell concentrations were determined as follows. Harvested bacteria samples (8 mL) were taken from the growth medium, centrifuged at 3000 rpm (model 228, Fisher Scientific), the supernatant was decanted, and the sample was resuspended in 8 mL of 0.17% aqueous NaCl. The washing step with 0.17% NaCl was repeated three times. The number of cells per unit volume was then counted by flow cytometry (model Epics XL-MCL, 488 nm; Beckman Coulter, Fullerton CA).

### 1.3 Pore Exclusion/Size Exclusion Chromatography

The chromatography system consisted of a biocompatible pump (Shimadzu, Columbia, MD), a high-pressure Teflon injection valve (model 9010, Rheodyne, Supelco, Bellefonte, PA), a Poros polycarbonate column, and a UV absorbance detector (model SPD-6A, Shimadzu). Column effluent was split with a PEEK microflow splitter (model P451, Upchurch Scientific, Oak Harbor, WA); 90% of the flow went to the UV detector, while 10% went to the nebulizer of the ICPMS device. The mobile phase consisted of 0.17% aqueous NaCl. This salt concentration was selected because the ionic strength was high enough to prevent cell lysis but low enough to minimize matrix effects and salt deposition in the ICPMS. Before use, the chromatographic column was always rinsed with 10 column volumes of 1 mM disodium EDTA solution.

The stationary-phase packing (Poros 50 OH, PerSeptive Applied Biosystems, Framingham, MD) was poly(styrene-divinylbenzene) with a cross-linked polyhydroxylated polymer coating. The specific surface area<sup>22</sup> was  $70 \pm 5 \text{ m}^2 \text{ g}^{-1}$ , and the mechanical strength was 10 MPa (100 kg cm<sup>-2</sup> or 1400 psi). These particles have two kinds of pores: large pores (~0.5- $\mu\text{m}$  diameter) that pass completely through the beads and small pores (~400- $\text{\AA}$  diameter) within the through pores. A column (0.95 cm i.d.  $\times$  13.5 cm) was packed in-house as described previously.<sup>22</sup> The samples injected into this column or into the ICP were the same as those counted by flow cytometry (vide supra), except for the final dilution. After the three washing steps, the bacteria samples were reconstituted in only 1 mL of 0.17% NaCl. Thus, the cell concentrations in the samples injected onto the column or into the ICPMS device are expected to be 8 times higher than those counted by flow cytometry. After the

samples were removed from the broth, no additional cell growth or reproduction was observed over the course of the experiments.

#### 1.4 ICPMS and Sample Introduction

A magnetic sector instrument (Element 1, Thermo Finnigan, Bremen, Germany) was used to monitor  $^{24}\text{Mg}^+$ ,  $^{44}\text{Ca}^+$ , and  $^{238}\text{U}^+$ . During chromatographic measurements, medium resolution ( $m/\Delta m \sim 4000$ ) was necessary for Mg and Ca, and there was more than sufficient signal for  $\text{U}^+$ , so the slit width was simply kept at the medium resolution setting throughout. The mass analyzer hopped between these three ions by electrostatic scans at three separate settings of the magnetic field. For continuous measurement of just  $^{238}\text{U}^+$ , the device was operated at low resolution. Here, the slits were wider, so the sensitivity (i.e.,  $\text{U}^+$  count rate per unit concentration) was  $\sim 10$  times higher in low resolution than in medium resolution. ICP operating conditions (Table 1) were selected to maximize signal for  $^7\text{Li}^+$ ,  $^{115}\text{In}^+$ , and  $^{238}\text{U}^+$  during tuning and calibration of the mass range. The split column effluent was nebulized by a microconcentric nebulizer (model 20100, Elemental Scientific, Inc., Omaha, NE) operated near its natural uptake rate ( $\sim 100 \mu\text{L min}^{-1}$ ), which is the liquid uptake due to the suction produced by the gas flow from the nebulizer tip. The aerosol then passed through a small Teflon double-pass spray chamber ( $25^\circ \text{C}$ , volume  $\sim 110 \text{ cm}^3$ ) and to the ICP.

## 2 Results and discussion

### 2.1 Chromatograms

Figures 1 and 2 show element-selective chromatograms obtained from two samples of *B. subtilis*. One sample was grown in "blank" or uranium-free culture medium and shows peaks for Mg and Ca but not U (Figure 1). A small chromatographic peak for Mg is evident

at ~200 s, which is attributed to Mg in cells. Chromatograms with UV absorbance detection and microscopic examination of collected fractions (data not shown) also indicate that the cells elute at ~200 s. The second Mg peak at ~450 s represents Mg from small molecules in solution. A Ca peak also appears at this latter time, but there is not enough Ca to see it in the cells. The sensitivity for Ca is much lower than that for Mg because of the low abundance of  $^{44}\text{Ca}$  (2.1%). A cool plasma<sup>29</sup> might allow use of the major Ca isotope ( $^{40}\text{Ca}$ ) but would not be useful for an element like U that forms refractory oxide ions.

The Mg chromatogram in Figure 2 shows peaks at the same retention times as before. However, the peak area for Mg in the cells (~200 s) is now much less than that for Mg in free solution (~450 s). Apparently, the incorporation of uranium by the cells reduces their binding with Mg. This observation shows the advantage of using a detector with multielement capabilities.

ICP Parameter	
outer gas flow rate	16 L min <sup>-1</sup>
nebulizer gas flow rate	0.94 L min <sup>-1</sup>
auxiliary gas flow rate	0.85 L min <sup>-1</sup>
rf power	1250 W
extraction lens voltage	-2000 V
focus lens voltage	-885 V
liquid flow rate (to nebulizer)	100 $\mu\text{L}$ min <sup>-1</sup>
spray chamber volume	110 cm <sup>3</sup>
spray chamber temperature	25 °C

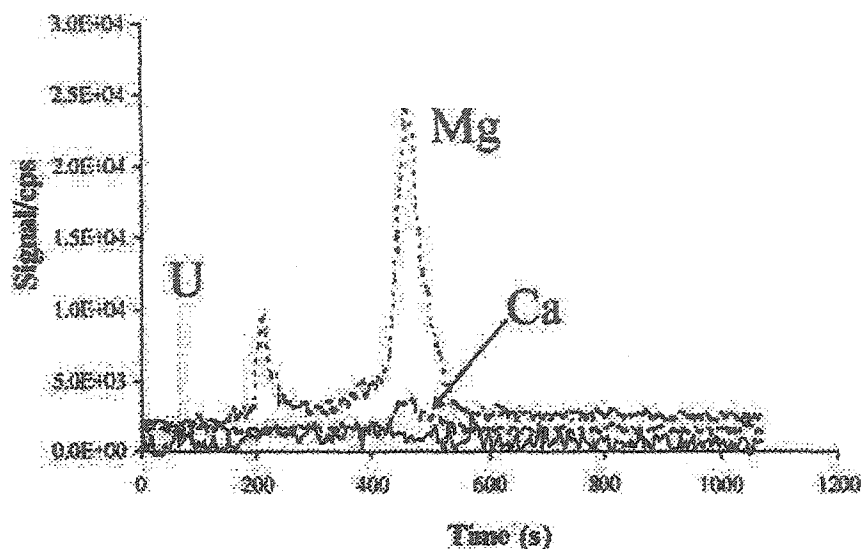


Figure 1. Element-selective chromatograms for *B. subtilis* grown in normal medium. Cell retention time is 200 s; small-molecule retention time is ~450 s under these conditions. This sample was incubated for 9 h; the cell concentration injected was  $\sim 6 \times 10^9$  cells  $\text{mL}^{-1}$ . The ICPMS monitors  $^{24}\text{Mg}^+$ ,  $^{44}\text{Ca}^+$ , and  $^{238}\text{U}^+$  at medium resolution.

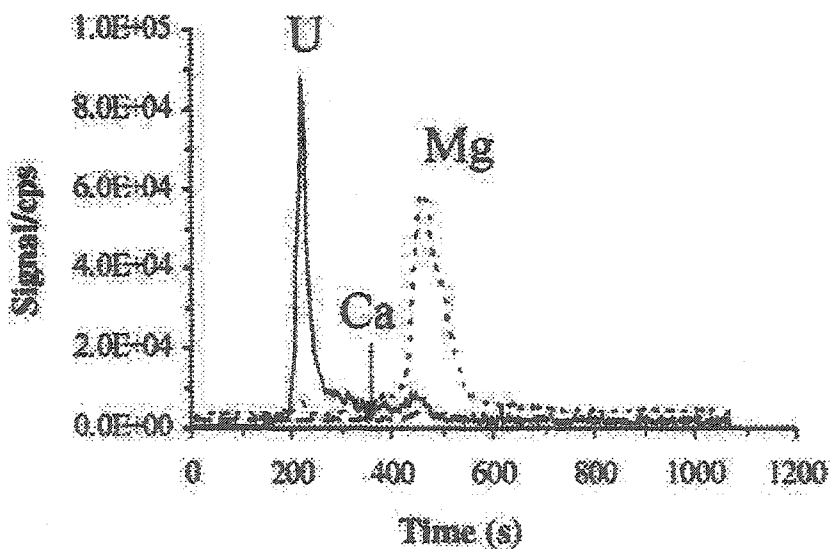


Figure 2. Chromatograms for *B. subtilis* cells cultured in medium spiked with uranium, obtained under the same conditions as in Figure 1. This sample was incubated for 24 h; the cell concentration injected was  $\sim 4 \times 10^9$  cells  $\text{mL}^{-1}$ . The ICPMS was operated at medium resolution.

## 2.2 Impact of Uranium on Cell Growth

Bacterial growth is generally described by four periods: lag, log, stationary, and death phases.<sup>30</sup> One question in the use of bacteria for remediating nuclear waste is whether exposure changes their growth behavior. To address this issue, *B. subtilis* cells were grown separately in the same media either with or without 14 ppm uranium. Each medium was sampled at different times, and the resulting cells were counted by flow cytometry.

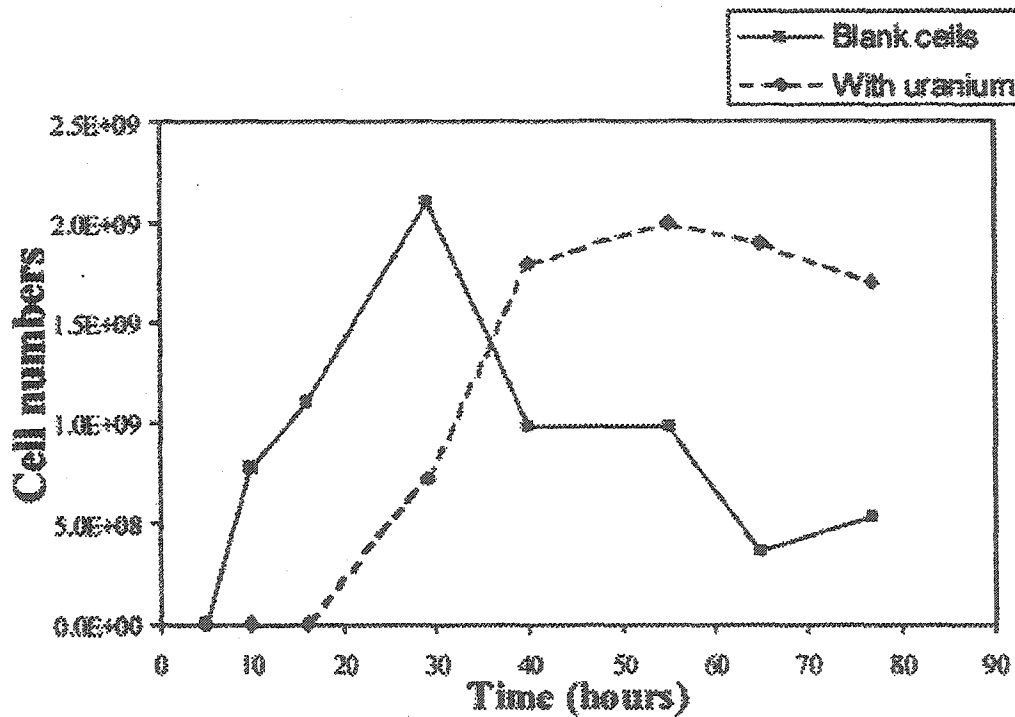


Figure 3. Growth curves for *B. subtilis* with uranium spike in culture medium (dashed line) and without uranium (solid line). Note the lag time for the onset of the log growth phase when uranium is present.

Figure 3 shows a plot of measured cell counts versus growth time for *B. subtilis*. For the normal medium, the cell counts maximize at 29 h and then decrease rapidly thereafter. For cells cultured in the uranium-spiked broth, 55 h is required to maximize cell concentration. Thus, the lag phase lasts longer with uranium present. Growth rate during the

log phase, i.e., the slope of the rising part of the curve, and maximum cell concentrations were about the same with or without uranium. Interestingly, the cells persist longer with uranium present.

The growth curve for *S. putrefaciens* (Figure 4) also has a longer lag phase with uranium present. However, the maximum cell concentration is only ~60% of that obtained in the absence of uranium. Thus, uranium exposure affects these two organisms differently. These general growth trends for both the normal and uranium-spiked growth media were reproduced four separate times over a two-week period.

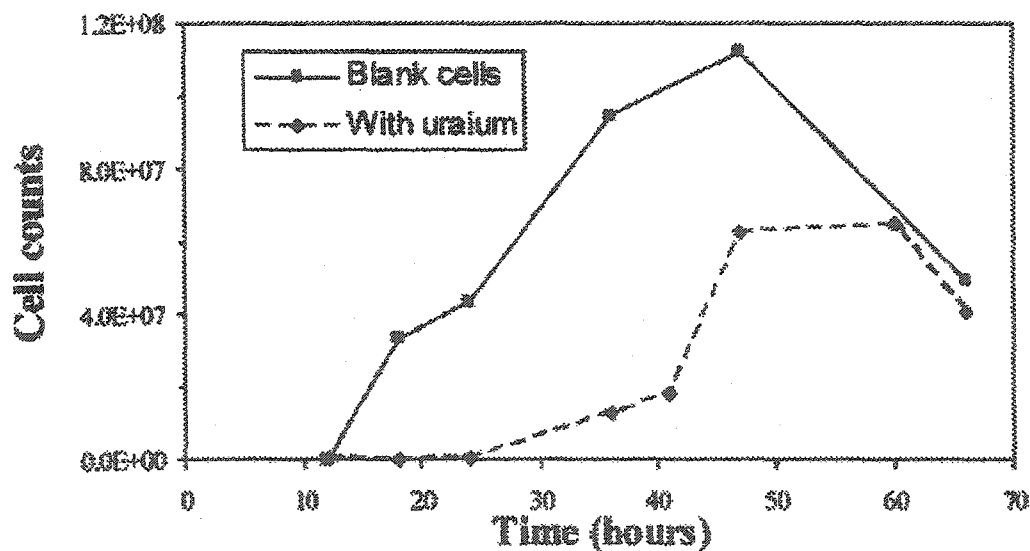


Figure 4. Growth curves for *S. putrefaciens* with uranium spike in culture medium (dashed line) and without uranium addition (solid line). Again note the delayed onset of the log growth phase as well as a decrease in overall cell numbers when uranium is present.

Figures 3 and 4 show growth curves only for the total cells. Uptake of uranium can also be monitored at various times. Figure 5 shows such results during growth of *B. subtilis*. The general shape of this curve is similar to that of Figure 3. Minor differences are that the



uranium content during the lag phase increases faster and uranium concentration during the death phase drops faster than the total cell counts. Note that measured uranium counts per individual cell did not change significantly during the incubation and growth period shown for *B. subtilis* (Figure 3, dashed line, and Figure 5). The variation in uranium counts per cell over the period from 20 to 80 h was  $\pm 14\%$ .

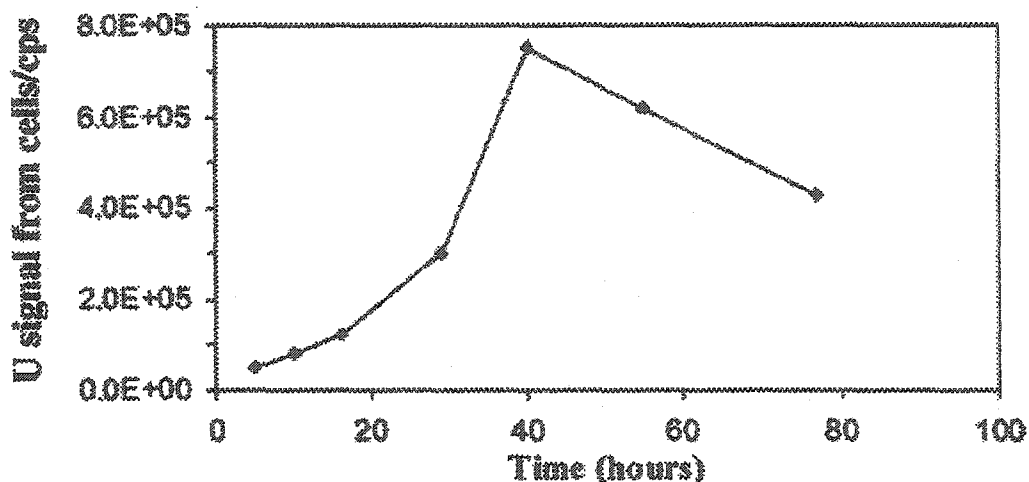


Figure 5. Uranium signal from *B. subtilis* cells during the fermentation process. Uranium signals were obtained from the first peak in the respective chromatograms (data not shown). The ICPMS was operated at low resolution, so the  $U^+$  sensitivity is  $\sim 10\times$  higher than that in the chromatograms of Figures 1 and 2.

### 2.3 Extrinsic versus Intrinsic Uranium

In the previous experiments, the uranium was present in the culture during cell growth and division. The washed cells isolated from this culture are said to contain "intrinsic" uranium. We also studied the extent to which the cells bind uranium if  $UO_2^{2+}$  is added only after the cells are removed from the culture. We call this uranium "extrinsic".

*B. subtilis* grown in normal medium was harvested during the log growth phase and divided into seven aliquots. These aliquots were added to buffer solutions containing 14 ppm

uranium so that each vial had  $1.2 \times 10^9$  cells  $\text{mL}^{-1}$ . After different time intervals, samples were injected from each vial onto the column.

Figure 6 shows the effect of exposure time on uranium signal from the cell fraction. These signals arise from extrinsically added uranium, i.e., uranium added only after the cells were grown and isolated. The cells adsorb uranium quickly and saturate after only  $\sim 10$  min. The  $\text{U}^+$  signal level is  $\sim 4 \times 10^4$  counts  $\text{s}^{-1}$ . In contrast, when cells are grown in broth spiked with uranium, the  $\text{U}^+$  signals are much higher,  $\sim 5 \times 10^5$  counts  $\text{s}^{-1}$  for the same cell count level. Thus, the cells bind substantially more uranium if it is present as they are grown.

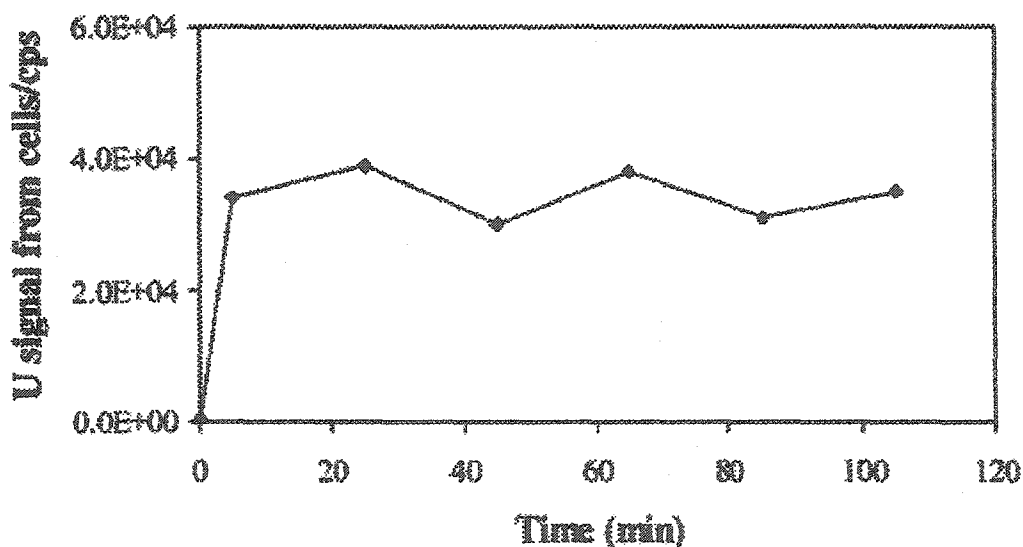


Figure 6. Extrinsic uranium in *B. subtilis*. Freshly cultured cells grown without uranium were suspended in 14 ppm uranium solution. All samples have same cell concentration ( $1.2 \times 10^9$  cells/mL) but different contact times with uranium solution. The ICPMS was operated in low resolution.

#### 2.4 Atomization of Cells in the ICP

It is interesting that cells generate metal ion signals from the ICP at all. They might be expected to behave like medium-sized wet droplets ( $\sim 2$ - $\mu\text{m}$  diameter) and pass through

the ICP intact or poorly dissociated.<sup>28</sup> Some indication of the extent of atomization in the ICP can be deduced from the time behavior of the signals in Figure 7. Although there is a definite steady-state level, the  $U^+$  signals from the cells are noisy, with occasional large spikes. In contrast, the uranium signal from a dissolved uranium standard is much more stable (Figure 7). Integrated signals measured for these plots exceed  $10^6$  counts, so the noise levels are well above counting statistics or shot noise.

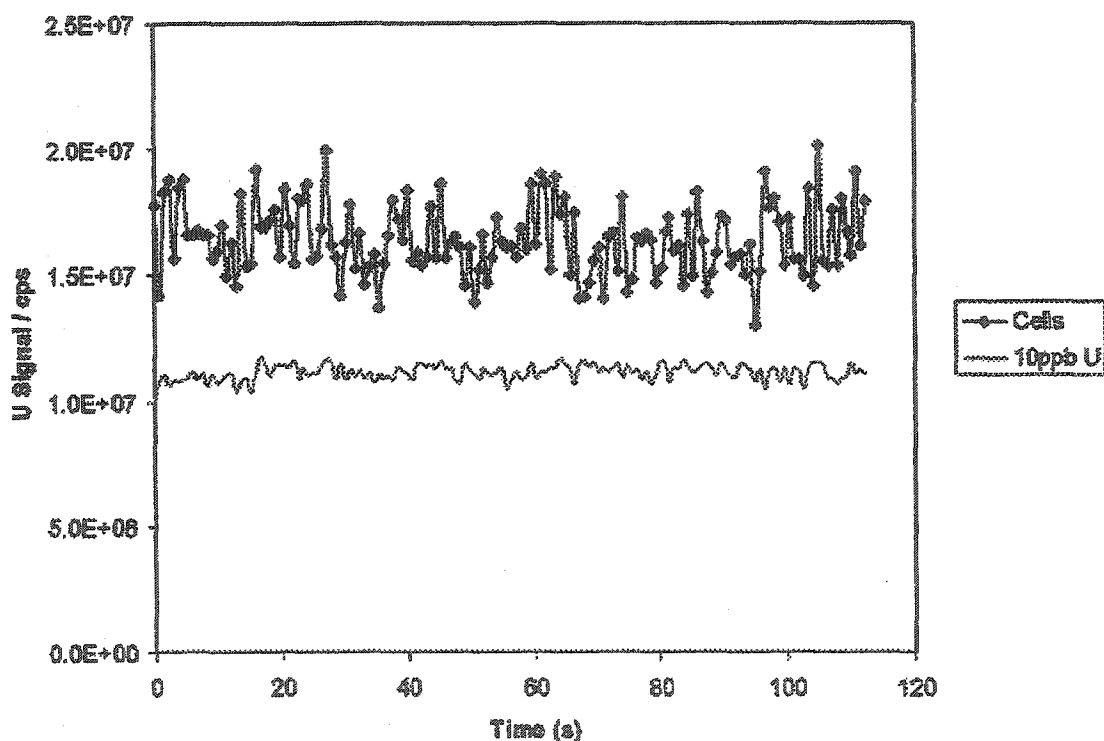


Figure 7. Comparison of noise behavior  $^{238}U^+$  signals from *B. subtilis* cells (in 0.17% NaCl) with  $U^+$  signals from 10 ppb dissolved uranium. The ICPMS device was operated in low resolution, and the samples were nebulized continuously.

Incomplete atomization of cells in the ICP is a likely cause of the noisy behavior seen in Figure 7. For example, a bacterium containing uranium that happens to atomize just in front of the sampler generates a high signal or a spike, whereas one that survives longer

depresses the signal. It is also possible that the spray generated by the nebulizer is less stable when cells pass through it.

### Conclusions

Pore exclusion/size exclusion chromatography coupled to ICPMS is an effective approach to rapidly isolate intact microorganisms from large and small molecules and to determine the elemental composition of each fraction. Uranium uptake by *B. subtilis* and *S. putrefaciens* takes two forms. The first and dominant form is intrinsic incorporation of the uranium during the development and growth of the colony. The bacteria also bind uranium added extrinsically to the solution. This takes place rapidly ( $\leq 10$  min under the condition of this study) but accounts for less than 10% of the total uranium associated with these bacteria. The presence of uranium in the cell culture can alter the rate of cell growth and the total cell population in some cases. Noise in the  $U^+$  signal induced by cells in the ICP and procedures for quantification and for determining the binding strength of uranium in the cells are under further investigation. The combined pore exclusion/size exclusion chromatography-ICPMS method should also be useful for various applications that require monitoring of other metals in microorganisms.<sup>32-35</sup>

### Acknowledgments

The ICPMS device used was provided by the U.S. Department of Energy, Chemical and Biological Sciences Program, Office of Basic Energy Sciences, and by the Office of Defense Nuclear Nonproliferation, Office of Nonproliferation Research and Engineering,

**References**

1. Clegg, J. W.; Foley, D. D. *Uranium Ore Processing*; Addison-Wesley: Reading, PA, 1958.
2. Brawner, C. O., Ed. *1st Int. Conf. on Uranium Mine Waste Disposal*, Soc. of Mining Engineers of the Am. Inst. of Mining, Metallurgical and Petroleum Engineers: Vancouver, BC, 1980.
3. Haveman, S. A.; Pedersen, K. J. *Contam. Hydrol.* **2002**, *55*, 161-174.
4. Chellam, S.; Clifford, D. A. *J. Environ. Eng.* **2002**, *128*, 942-952.
5. Hara, K. *Proc. Sci. Meet. Environ. Health Phys.* **2000**, 109-129.
6. Faanhof, A.; Louw, I. J. *Radioanal. Nucl. Chem.* **2001**, *249*, 227-232.
7. Ferenbaugh, J. K.; Fresquez, P. R.; Ebinger, M. H.; Gonzales, G. J.; Jordan, P. A. *Environ. Monit. Assess.* **2002**, *74*, 243-254.
8. Domingo, J. L. *Reproductive Toxicol.* **2001**, *15*, 603-609.
9. Taylor, D. M.; Taylor, S. K. *Rev. Environ. Health* **1997**, *12*, 147-157.
10. Jacobs, S. A.; Schexnailder, S. J.; Urban, C.; Smith, T. C.; Gonzales, D. E. Society of Mining Engineers of the American Institute of Mining, Metallurgical, and Petroleum Engineers, Inc.; Vancouver, BC 1980; pp 361-364.
11. Al-Attar, L.; Dyer, A.; Blackburn, R. *J. Radioanal. Nucl. Chem.* **2000**, *246*, 451-455.
12. Michard, P.; Guibal, E.; Vincent, T.; Le Cloirec, P. *Microporous Mater.* **1996**, *5*, 309-324.
13. Garcia, R.; Pinel, C.; Madic, C.; Lemaire, M. *Tetrahedron Lett.* **1998**, *39*, 8651-8654.
14. Saunders, G. D.; Foxon, S. P.; Walton, P. H.; Joyce, M. J.; Port, S. N. *Chem. Commun.* **2000**, *4*, 273-274.
15. Riordan, C.; Bustard, M.; Putt, R.; McHale, A. P. *Biotechnol. Lett.* **1997**, *19*, 385-387.

16. Mohagheghi, A.; Updegraff, D. M.; Goldhaber, M. B. *Geomicrobiol. J.* **1985**, *4*, 153-173.
17. Hu, M. Z.-C.; Reeves, M. *Biotechnol. Prog.* **1997**, *13*, 60-70.
18. Beveridge, T. J.; Meloche, J. D.; Fyfe, W. S.; Murray, R. G. E. *Appl. Environ. Microbiol.* **1983**, *45*, 1094-1108.
19. Haas, J. R.; Dichristina, T. J.; Wade, R., Jr. *Chem. Geol.* **2001**, *180*, 33-54.
20. Nakajima, A.; Sakaguchi, Takashi *Appl. Microbiol. Biotechnol.* **1986**, *24*(1), 59-64.
21. Strandberg, G. W.; Shumate, S. E., II; Parrott, J. R., Jr. *Appl. Environ. Microbiol.* **1981**, *41*, 237.
22. Berthod, A.; Zhang, B.; Armstrong, D. W. *J. Sep. Sci.* **2003**, *26*, 20-28.
23. Wang, J.; Houk, R. S.; Dreessen, D.; Wiederin, D. R. *J. Biol. Inorg. Chem.* **1999**, *4*, 546-553.
24. Wang, J.; Dreessen, D.; Wiederin, D. R.; Houk, R. S. *J. Am. Chem. Soc.* **1998**, *120*, 5793-5799.
25. Fowle, D. A.; Fein, J. B. *Chem. Geol.* **2000**, *168*, 27-36.
26. Fredrickson, J. K.; Zachara, J. M.; Kennedy, D. W.; Duff, M. C.; Gorby, Y. A.; Li, S.-M. W.; Krupka, K. M. *Geochim. Cosmochim. Acta* **2000**, *64*, 3085-3098.
27. Rajan, K. S.; Martell, A. E. *Inorg. Chem.* **1965**, *4*, 462-469.
28. Viragh, K.; Szolnoki, J. *Foldt. Kozl.* **1970**, *100*, 43.
29. Patterson, K. Y.; Veillon, C.; Hill, A. D.; Moser-Veillon, P. B.; O'Haver, T. C. *J. Anal. At. Spectrom.* **1999**, *14*, 1673-1677.
30. Ingraham, J. L.; Ingraham, C. A. *Introduction to Microbiology*, 2nd ed.; Brooks/Cole: Pacific Grove, CA, 2000.
31. Houk, R. S.; Winge, R. K.; Chen, X. S. *J. Anal. At. Spectrom.* **1997**, *12*, 1139-1148.

32. Cuero, R.; Ouellet, T.; Yu, J.; Mogongwa, N. *J. Appl. Microbiol.* **2003**, *94*, 953-961.
33. Holden, J. F.; Adamns, M. W. W. *Curr. Opin. Chem. Biol.* **2003**, *7*, 160-165.
34. Cavet, J. S.; Barrelly, G. P. M.; Robinson, N. J. *FEMS Microbiol. Rev.* **2003**, *27*, 165-181.
35. Zhang, Y.; Zhang, Z.; Suzuki, K.; Maekawa, T. *Biomass Bioenergy* **2003**, *25*, 427-433.

## GENERAL CONCLUSIONS

Macrocyclic glycopeptide CSPs are a class of widely used chiral selectors. Since these chiral selectors are structurally related, they tend to have the similar, but not identical, enantioselectivity for most compounds. Two classes of chiral compounds, oxazolidinones and dansylated amino acids, were found to have reversed elution orders when separated by different macrocyclic glycopeptide CSPs. The D-dansyl amino acids are retained longer on the vancomycin and teicoplanin CSPs, while the L-enantiomers are more retained on ristocetin A CSP. No general trend of the elution order reversal was found for oxalidinones.

Macrocyclic glycopeptide CSPs have great resolving power for closely related peptides separated by HPLC. In general: (1) terminal single amino acid polymorphisms produced separations of greater resolution than those occurring in the middle of the peptide, (2) substituting a charged amino acid for an uncharged residue produced a separation of greater resolution than exchanging an uncharged amino acid for another uncharged amino acid or substituting like charged amino acids, and (3) All peptides containing a D-amino acid polymorphism eluted before the corresponding L-amino acid containing peptide. Most of the mobile phase conditions used are MS-compatible and good LOD can be achieved by using ESI/MS. The retention behavior of peptides on macrocyclic glycopeptide CSPs shows U-curve shaped retention versus the concentration of the organic modifier content. Mobile phase composition, including the type and amount of organic modifier, mobile phase pH, and ionic strength, plays important roles in peptide elution behavior and peak shape. The selectivity of the macrocyclic glycopeptide stationary phases for achiral and chiral



polymorphisms using ESI-MS compatible mobile phases should broaden their appeal for use in all areas where peptide separations are important.

The perfusion polystyrene divinyl benzene packing material with spherical polar particles, large throughpores and small pores, can be used to quickly separate large microorganisms by total exclusion from the macromolecules and from the small molecules that penetrate the porous spheres. It is noted that microorganisms give a negative response with polarimetric detection while most natural optically active small molecules and macromolecules give a positive response. This can be used to selectively detect and quantitate microorganisms. The combination of perfusion chromatography with polarimetric detection can accelerate the real time monitoring and control of industrial fermentation broths.

Pore exclusion/size exclusion chromatography coupled to ICPMS is an effective approach to rapidly isolate intact microorganisms from large and small molecules and to determine the elemental composition of each fraction. Uranium uptake by *B. subtilis* and *S. putrefaciens* takes two forms. The first and dominant form is intrinsic incorporation of the uranium during the development and growth of the colony. The bacteria also bind uranium added extrinsically to the solution. This takes place rapidly (10 min under the conditions of this study) but accounts for less than 10% of the total uranium associated with these bacteria. The presence of uranium in the cell culture can alter the rate of cell growth and the total cell population in some cases. The combined pore exclusion/size exclusion chromatography-ICPMS method should also be useful for various applications that require monitoring of other metals in microorganisms.

In Chapter 2, my contributions involved the oxazolidione separations and a few dansyl amino acid separations. In chapter 3, my contributions involved the peptide separations on Chirobiotic T and TAG columns, as well as the detection comparison between ESI/MS and UV, and the detection linearity study. In chapter 5, 6, I contributed the most of work.

## ACKNOWLEDGEMENTS

The studies carried out in this dissertation were under Professor Armstrong's supervision and support. Professor Houk also provided me with guidance in many studies done in this dissertation. During these years, I received generous assistance from our research group members, visiting scholars and collaborate researchers. Iowa State University chemistry department, Department of Energy Ames Laboratory and University of Missouri Rolla chemistry department also provided me support. Without all this guidance and support, it would have been impossible for me to finish this study. I sincerely thank everyone.